Low-Complexity ICI Mitigation Methods for High-Mobility SISO/MIMO-OFDM Systems

Chao-Yuan Hsu, *Student Member, IEEE*, and Wen-Rong Wu, *Member, IEEE*

Abstract—In orthogonal frequency-division multiplexing (OFDM) systems, it is generally assumed that the channel response is static in an OFDM symbol period. However, the assumption does not hold in high-mobility environments. As a result, intercarrier interference (ICI) is induced, and system performance is degraded. A simple remedy for this problem is the application of the zero-forcing (ZF) equalizer. Unfortunately, the direct ZF method requires the inversion of an $N \times N$ ICI matrix, where N is the number of subcarriers. When N is large, the computational complexity can become prohibitively high. In this paper, we first propose a low-complexity ZF method to solve the problem in single-input–single-output (SISO) OFDM systems. The main idea is to explore the special structure inherent in the ICI matrix and apply Newton's iteration for matrix inversion. With our formulation, fast Fourier transforms (FFTs) can be used in the iterative process, reducing the complexity from $\mathcal{O}(N^3)$ to $\mathcal{O}(N \log_2 N)$. Another feature of the proposed algorithm is that it can converge very fast, typically in one or two iterations. We also analyze the convergence behavior of the proposed method and derive the theoretical output signal-to-interference-plus-noise ratio (SINR). For a multiple-input–multiple-output (MIMO) OFDM system, the complexity of the ZF method becomes more intractable. We then extend the method proposed for SISO-OFDM systems to MIMO-OFDM systems. It can be shown that the computational complexity can be reduced even more significantly. Simulations show that the proposed methods perform almost as well as the direct ZF method, while the required computational complexity is reduced dramatically.

Index Terms—Fast Fourier transform (FFT), intercarrier interference (ICI), Newton's iteration.

I. INTRODUCTION

ORTHOGONAL frequency-division multiplexing (OFDM) is known to be a successful technique for coping with the multipath channel effect in wireless communications [1]. For conventional OFDM systems, it is usually assumed that the channel is static in an OFDM symbol period. However, in high-speed mobile environments, this assumption no longer holds. If the channel is time variant in an OFDM symbol period, orthogonality will be destroyed. Intercarrier interference (ICI) is induced, and system performance is degraded. The behavior of mobility-induced ICI has been extensively investigated in the literature [2]–[7]. In [2] and [3], it is shown that the interference on a subcarrier mainly comes from neighboring

subcarriers. In addition, the interference level is proportional to the Doppler frequency.

Many techniques have been developed to solve the mobility-induced ICI problem. Two algorithms are well known, namely, 1) the zero-forcing (ZF) method and 2) the minimum mean square error (MMSE) equalization method. Unfortunately, these methods require the inversion of an $N \times N$ ICI matrix, where N is the number of subcarriers. When N is large, the required computational complexity becomes high. Systems with a lot of subcarriers are not uncommon in real-world applications. For example, for the application of digital video broadcasting (DVB), the number of subcarriers can be as large as 8192. To solve the problem, a simpler ICI equalizer for the ZF method was developed in [8]. As mentioned, ICI on a subcarrier mainly comes from a few neighboring subcarriers. Thus, ICI from other subcarriers can then be ignored. This method has good performance in low-mobility environments. In high-mobility environments, however, the number of insignificant ICI terms will be decreased, and the computational complexity will be significantly increased.

Successive interference cancellation (SIC) and parallel interference cancellation (PIC) are two well-known multiuser interference (MUI) cancellation techniques in code-division multiple-access systems. Since the characteristic of ICI is similar to that of MUI, these methods can be directly applied to ICI suppression in OFDM systems. A method that combines the MMSE method and SIC was first proposed in [9]. Later, it was improved with a recursive method in [10], reducing the required complexity further. Although good performance can be achieved with these methods, the required complexity is still high, and the time delay can be intolerably large. The PIC technique was then employed to solve the problem [11]–[15]. Although the processing delay is greatly reduced, the performance is discounted as well. Other approaches use transmitter frequency-domain coding or beamforming to reduce ICI or to enhance the received signal-to-interference-plus-noise ratio (SINR). Interested readers are referred to [16]–[19].

Apart from the processing in the frequency domain, some researchers also explore that in the time domain. In [20], a time-domain filtering technique, maximizing the signal-to-ICI-plus-noise ratio, was proposed for single-input–single-output (SISO)/multiple-input–multiple-output (MIMO) OFDM systems. One disadvantage of this method is that it requires matrix operations to solve a generalized eigenvalue problem. Another approach involves the use of a time-variant time-domain equalizer, making the time-variant channel less variant. Transferring the equalizer from time domain to frequency domain, one can obtain a frequency-domain per-tone equalizer (PTEQ).

The PTEQ was originally proposed to deal with the insufficient cyclic prefix (CP) problem in OFDM systems. Lately, it has been extended to suppress ICI in SISO/MIMO-OFDM systems [21]–[25]. The PTEQ is well known for its good performance; however, its implementation complexity and storage requirement can be high. In [26], a two-stage equalizer was proposed. In the first stage, a time-domain windowing technique is used to shorten the ICI response in the frequency domain. In the second stage, an iterative MMSE method is used to suppress the residual ICI. Although the windowing approach is simple, the iterative MMSE processing is not trivial.

As mentioned, the main problem in the ZF method is the matrix inversion. Thus, conducting this operation efficiently becomes the main concern. It is found that some iterative methods can be much more efficient than the direct inversion method. In [27], the Gauss–Seidel iteration was used to conduct the matrix inversion. However, it still needs a matrix inverse in its iterative process. Another method, called operator perturbation, was recently proposed [28]. Similar to [27], this method also requires a matrix inverse in its iterations. Thus, the computational complexity for the methods in [27] and [28] is still high. In [30], it was discovered that the ICI matrix for a linear time-variant (LTV) channel model exhibits a special structure, allowing the application of fast Fourier transforms (FFTs) in the matrix inversion. The LTV channel model was proposed in [8], and it is originally designed for time-variant channel estimation [29]. Exploiting this structure, Fu *et al.* [30] proposed a power-series expansion (PSE) method for the ICI matrix inversion. Although the PSE method can greatly reduce the computational complexity, it does not perform well in high-mobility environments.

In this paper, we propose a low-complexity ZF method to solve the mobility-induced ICI problem in SISO-OFDM [32] and MIMO-OFDM systems. Similarly to [30], we exploit the special structure inherent in the LTV channel model. We first develop a method that can implement Newton's iteration for the ICI matrix inversion in SISO-OFDM systems. With our specially designed architecture, FFTs can be used, reducing the computational complexity effectively. We also propose a method for the calculation of initial values. With those values, Newton's iteration can converge very fast, usually within a couple of iterations. Unlike the PSE method [30], our method works well even in high-mobility environments. Simulation results show that the performance of the proposed low-complexity ZF method can be as good as that of the direct ZF method. However, the required computational complexity is reduced from $\mathcal{O}(N^3)$ to $\mathcal{O}(N \log_2 N)$. We also analyze the convergence behavior of the proposed low-complexity ZF algorithm and derive the theoretical output SINR. With a new MIMO-OFDM system formulation, we then extend the proposed method to ICI suppression in MIMO-OFDM systems. It is shown that in MIMO-OFDM systems, the computational complexity can be reduced even more significantly. For an $M \times M$ system, where M is the number of transmit (receive) antennas, the proposed algorithm can reduce the computational complexity from $\mathcal{O}(M^3 N^3)$ to $\mathcal{O}(MN \log_2 N)$.

The rest of this paper is organized as follows. Section II presents the proposed ICI mitigation method for SISO-OFDM systems. Section III describes the proposed ICI cancellation method for MIMO-OFDM systems. Section IV conducts the performance analysis. Simulation results are reported in Section V, demonstrating the effectiveness of the proposed method. Finally, conclusions are drawn in Section VI.

II. ICI MITIGATION FOR SISO-OFDM

A. ZF Method

Consider a mobile OFDM system whose channel variation is large such that the mobility-introduced ICI cannot be ignored. It was shown in [29] that the LTV channel model can be used to approximate a time-variant channel for normalized Doppler frequency up to 20%, where the normalized Doppler frequency is defined as the maximum Doppler frequency divided by subcarrier spacing. Using the LTV channel model, we can approximate the time-variant channel in a specific OFDM symbol period as

$$h_j(n) = h_{0,j} + n \times h_{1,j} \tag{1}$$

where n is the time index, $h_j(n)$ is the jth-tap channel response at time instant n, $h_{0,j}$ is its constant term, and $h_{1,j}$ is its variation slope. We assume that n is 0 at the midpoint of an OFDM symbol. Let $\mathbf{h}_0 = [h_{0,0}, h_{0,1}, \ldots, h_{0,N-1}]^T$, $\mathbf{h}_1 = [h_{1,0}, h_{1,1}, \ldots, h_{1,N-1}]^T$, $\mathbf{H}_0 = cir(\mathbf{h}_0)$, and $\mathbf{H}_1 = cir(\mathbf{h}_1)$, where $cir(\mathbf{c})$ denotes a circulant matrix with the first column vector being $\mathbf{c}$. In addition, we define $\mathbf{v}_1 = [(-N+1)/2, (-N+3)/2, \ldots, (N-1)/2]^T$ and $\mathbf{V}_1 = \text{diag}(\mathbf{v}_1)$, where the notation $\text{diag}(\mathbf{d})$ denotes a diagonal matrix with the diagonal vector of $\mathbf{d}$. According to (1), we can express the received time-domain signal in the OFDM symbol (after CP removal) as

$$\mathbf{y} = (\mathbf{H}_0 + \mathbf{V}_1 \mathbf{H}_1)\mathbf{x} + \mathbf{z} \tag{2}$$

where $\mathbf{y}$ and $\mathbf{x}$ are the receive and transmit time-domain signals, respectively, and $\mathbf{z}$ is the noise vector (additive white Gaussian). Let $\mathbf{G}$ be a unitary discrete Fourier transform (DFT) matrix with the property that $\mathbf{G}\mathbf{G}^H = \mathbf{I}_N$, where $\mathbf{I}_N$ is an $N \times N$ identity matrix. Furthermore, let $\widetilde{\mathbf{y}} = \sqrt{N}\mathbf{G}\mathbf{y}$, $\widetilde{\mathbf{x}} = \sqrt{N}\mathbf{G}\mathbf{x}$, $\widetilde{\mathbf{z}} = \sqrt{N}\mathbf{G}\mathbf{z}$, $\widetilde{\mathbf{h}}_0 = \sqrt{N}\mathbf{G}\mathbf{h}_0$, $\widetilde{\mathbf{h}}_1 = \sqrt{N}\mathbf{G}\mathbf{h}_1$, $\widetilde{\mathbf{H}}_0 = \text{diag}(\widetilde{\mathbf{h}}_0)$, and $\widetilde{\mathbf{H}}_1 = \text{diag}(\widetilde{\mathbf{h}}_1)$. Multiplying both sides of (2) by $\sqrt{N}\mathbf{G}$, we can express the receive signal in the frequency domain as

$$\begin{aligned} \widetilde{\mathbf{y}} &= [\widetilde{\mathbf{H}}_0 + \mathbf{G}\mathbf{V}_1\mathbf{G}^H\widetilde{\mathbf{H}}_1]\widetilde{\mathbf{x}} + \widetilde{\mathbf{z}} \\ &= \widetilde{\mathbf{M}}\widetilde{\mathbf{x}} + \widetilde{\mathbf{z}} \end{aligned} \tag{3}$$

where $\widetilde{\mathbf{M}} = \widetilde{\mathbf{H}}_0 + \mathbf{G}\mathbf{V}_1\mathbf{G}^H\widetilde{\mathbf{H}}_1$. Note that $\widetilde{\mathbf{M}}$ can also be rewritten as $\widetilde{\mathbf{M}} = \widetilde{\mathbf{H}}_0 + \widetilde{\mathbf{V}}_1\widetilde{\mathbf{H}}_1$, where $\widetilde{\mathbf{V}}_1 = \mathbf{G}\mathbf{V}_1\mathbf{G}^H = [cir(\widetilde{\mathbf{v}}_1)]^T$ and $\widetilde{\mathbf{v}}_1 = (1/\sqrt{N})\mathbf{G}^H\mathbf{v}_1$.

Denote the ZF equalized signal as $\overline{\mathbf{x}}_{ZF}$. Then, we can have $\overline{\mathbf{x}}_{ZF} = \widetilde{\mathbf{M}}^{-1}\widetilde{\mathbf{y}}$. From the above formulation, it is simple to see that direct implementation of the ZF method will require high computational complexity if N is large. The PSE method was

introduced in [30] to solve the problem. The idea is to express $\widetilde{\mathbf{M}}^{-1}$ as

$$
\widetilde{\mathbf{M}}^{-1} = \left[\left(\mathbf{I}_N + \mathbf{G}\mathbf{V}_1\mathbf{G}^H\widetilde{\mathbf{H}}_1\widetilde{\mathbf{H}}_0^{-1} \right) \widetilde{\mathbf{H}}_0 \right]^{-1}
$$
$$
= \widetilde{\mathbf{H}}_0^{-1}(\mathbf{I}_N - \mathbf{P})^{-1} \qquad (4)
$$

where $\mathbf{P} = \mathbf{G}\mathbf{V}_1\mathbf{G}^H\overline{\mathbf{H}}$ and $\overline{\mathbf{H}} = -\widetilde{\mathbf{H}}_1\widetilde{\mathbf{H}}_0^{-1}$. Then, $(\mathbf{I}_N - \mathbf{P})^{-1}$ is expanded with a power series, and high-order terms are truncated, i.e., $(\mathbf{I}_N - \mathbf{P})^{-1} \approx \sum_{i=0}^{Q} \mathbf{P}^i$, where Q is the highest order retained in the expansion. The convergence condition for this expansion is that $\|\mathbf{P}\| < 1$ [30], where $\|\mathbf{P}\|$ indicates the p-norm of $\mathbf{P}$ [31]. Finally, the equalized $\widetilde{\mathbf{x}}$, which is denoted as $\overline{\mathbf{x}}_{PSE}$, is equal to $\widetilde{\mathbf{H}}_0^{-1} \sum_{i=0}^{Q} \mathbf{a}_i$, where $\mathbf{a}_i = \mathbf{P}^i\widetilde{\mathbf{y}}$. Note that $\mathbf{a}_{i+1} = \mathbf{P}\mathbf{a}_i = \mathbf{G}\mathbf{V}_1\mathbf{G}^H(\overline{\mathbf{H}}\mathbf{a}_i)$. Thus, $\mathbf{a}_i$ can be recursively calculated. Furthermore, with the special structure of $\mathbf{P}$, FFTs/inverse FFTs (IFFTs) can be used to calculate $\mathbf{a}_i$. Although the computational complexity can be reduced effectively, the performance of the PSE method is unsatisfactory in high-mobility environments. In Section II-B, we will present the proposed method to solve the problem.

B. Proposed ICI Mitigation Method

As mentioned, the PSE method is unsatisfactory in high-mobility environments. To solve the problem, we seek for a more powerful iterative method for matrix inversion. Specifically, we find that Newton's iteration is useful. Newton's iteration is well known for its fast convergence [33], [34] and has been investigated extensively [35]–[38]. Let $\mathbf{W}_k$ be the estimated inverse of $\widetilde{\mathbf{M}}$ at the kth iteration. The $(k+1)$th Newton's iteration can be described as follows:

$$
\mathbf{W}_{k+1} = (2\mathbf{I}_N - \mathbf{W}_k\widetilde{\mathbf{M}})\mathbf{W}_k, \qquad k = 0, 1, 2, \ldots, \infty. \quad (5)
$$

Let $\widetilde{\mathbf{R}}_k = \mathbf{I}_N - \mathbf{W}_k\widetilde{\mathbf{M}}$ represent the estimation residual. Equation (5) implies that $\|\mathbf{I}_N - \mathbf{W}_k\widetilde{\mathbf{M}}\| \le \|\mathbf{I}_N - \mathbf{W}_0\widetilde{\mathbf{M}}\|^{2^k}$ for all k. If $\|\mathbf{I}_N - \mathbf{W}_0\widetilde{\mathbf{M}}\| < 1$, we then have a quadratic convergence [39]. From (5), we can clearly see that Newton's iteration requires matrix-to-matrix multiplications whose computational complexity is high. As a matter of fact, its complexity is even higher than that of the direct ZF method when k is large. Thus, a direct application of Newton's iteration for matrix inversion is not feasible. In what follows, we propose a method of solving the problem.

Iterating (5), we obtain a sequence of matrices $\{\mathbf{W}_0, \mathbf{W}_1, \ldots, \mathbf{W}_k\}$. The relationship between $\mathbf{W}_0$ and $\mathbf{W}_k$ can be found straightforwardly in

$$
\mathbf{W}_k = \sum_{m=0}^{2^k-1} \overline{c}_{k,m}(\mathbf{W}_0\widetilde{\mathbf{M}})^m\mathbf{W}_0 \qquad (6)
$$

where $\overline{c}_{k,m}$ is the coefficient of the mth summation term in (6). Equation (6) can be seen as an expansion form of Newton's iteration, while (5) is an iterative form. It turns out that to obtain a low-complexity algorithm, we have to use the expansion form. Assign $\overline{c}_{k,m}$'s as coefficients of a polynomial function of z, i.e., $f_k(z) = \overline{c}_{k,0}z^0 + \overline{c}_{k,1}z^1 + \cdots + \overline{c}_{k,2^k-1}z^{2^k-1}$.

Then, the polynomial $f_{k+1}(z)$ can be derived from $f_k(z)$ as $f_{k+1}(z) = 2f_k(z) - z[f_k(z)]^2$, where $f_0(z) = 1$. This is to say that $\overline{c}_{k,m}$ can be recursively calculated. Note that our objective is to obtain the equalized result $\mathbf{W}_k\widetilde{\mathbf{y}}$ and not the matrix inverse $\mathbf{W}_k$ itself. By multiplying both sides of (6) by $\widetilde{\mathbf{y}}$ and letting $\overline{\mathbf{x}}_k = \mathbf{W}_k\widetilde{\mathbf{y}}$ and $\overline{\mathbf{u}}_m = (\mathbf{W}_0\widetilde{\mathbf{M}})^m\mathbf{W}_0\widetilde{\mathbf{y}}$, we have the equalized result as

$$
\overline{\mathbf{x}}_k = \sum_{m=0}^{2^k-1} \overline{c}_{k,m}\overline{\mathbf{u}}_m. \qquad (7)
$$

From the definition of $\overline{\mathbf{u}}_m$, we can then have

$$
\overline{\mathbf{u}}_{m+1} = (\mathbf{W}_0\widetilde{\mathbf{M}})\overline{\mathbf{u}}_m. \qquad (8)
$$

As a result, $\overline{\mathbf{u}}_m$ can be recursively calculated as well. Using this approach, we have transformed matrix-to-matrix multiplications in (6) into matrix-to-vector multiplications in (7) and (8).

To complete our low-complexity algorithm, we make use of the special structure inherent in the ICI matrix. From the foregoing derivation, we know that $\widetilde{\mathbf{M}} = \widetilde{\mathbf{H}}_0 + \mathbf{G}\mathbf{V}_1\mathbf{G}^H\widetilde{\mathbf{H}}_1$. By using this structure, we can then rewrite (8) as

$$
\overline{\mathbf{u}}_{m+1} = \left[\mathbf{W}_0(\widetilde{\mathbf{H}}_0 + \mathbf{G}\mathbf{V}_1\mathbf{G}^H\widetilde{\mathbf{H}}_1) \right] \overline{\mathbf{u}}_m
$$
$$
= \mathbf{W}_0 \left[\widetilde{\mathbf{H}}_0\overline{\mathbf{u}}_m + \mathbf{G}\mathbf{V}_1\mathbf{G}^H(\widetilde{\mathbf{H}}_1\overline{\mathbf{u}}_m) \right]. \qquad (9)
$$

Note that $\widetilde{\mathbf{H}}_0$, $\widetilde{\mathbf{H}}_1$, and $\mathbf{V}_1$ are all diagonal matrices. If we further pose a constraint that $\mathbf{W}_0$ is a diagonal matrix, we can transform matrix-to-matrix operations into vector-to-vector and DFT/IDFT operations, as shown in (9). As known, DFTs/IDFTs can be efficiently implemented with FFTs/IFFTs whose complexity is $\mathcal{O}(N \log_2 N)$. Thus, the computational complexity of the proposed algorithm is $\mathcal{O}(N \log_2 N)$. The constraint on $\mathbf{W}_0$ may not always yield satisfactory performance in all scenarios. Instead of a diagonal matrix, we may let $\mathbf{W}_0$ be a low-bandwidth banded matrix. Let the (i,j)th entry of a matrix $\mathbf{B}$ be denoted as $\mathbf{B}(i,j)$. The banded matrix is defined as $\mathbf{B}(i,j) \ne 0$, if $|i - j| \le D$, and $\mathbf{B}(i,j) = 0$, otherwise. Here, D is the bandwidth of the banded matrix. If $D = 0$, the banded matrix is reduced to a diagonal matrix. If $D = 1$, the matrix will have three nonzero diagonal vectors. With this type of $\mathbf{W}_0$, the computational complexity in (9) will only be increased slightly. For later simulations, we will only consider the cases of $D = 0$ and $D = 1$. It turns out that for $D = 1$, the performance of the proposed algorithm is good enough.

The final thing we have to deal with is how to determine the initial matrix $\mathbf{W}_0$. A good initial matrix can reduce the number of iterations significantly and provide good cancellation performance. As known, the main function of ZF is to invert the ICI matrix, and in the ideal case, $\mathbf{I}_N - \mathbf{W}_k\widetilde{\mathbf{M}} = \mathbf{0}_N$, where $\mathbf{0}_N$ is an $N \times N$ zero matrix. As a result, if $\mathbf{I}_N - \mathbf{W}_0\widetilde{\mathbf{M}}$ can be made as close to $\mathbf{0}_N$ as possible, fast convergence in Newton's algorithm can be obtained. Based on this idea, we propose to minimize the Frobenius norm of $\mathbf{I}_N - \mathbf{W}_0\widetilde{\mathbf{M}}$, i.e.,

$$
\mathbf{W}_0 = \arg\min_{\mathbf{w}} \|\mathbf{I}_N - \mathbf{W}\widetilde{\mathbf{M}}\|_F^2 \qquad (10)
$$

TABLE I
COMPLEXITY COMPARISON AMONG N-ZF, PSE, AND DIRECT ZF METHODS IN A SISO-OFDM SYSTEM

Methods	Real multiplications	Real divisions	Real additions
Direct ZF	$\frac{4}{3}N^3 + 7N^2 - \frac{1}{3}N$	$N^2 + N$	$\frac{4}{3}N^3 + \frac{11}{2}N^2 - \frac{23}{6}N$
PSE	$4QN\log_2(N) + (6Q+12)N$	$4N$	$6QN\log_2(N) + (4Q+6)N$
N-ZF ($D=0$)	$(2^{k+2}-4)N\log_2(N)+[2^{k+4}+8S-8]N$	$2N$	$3(2^{k+1}-2)N\log_2(N)+[5\times2^{k+1}+8S-5]N$
N-ZF ($D=1$)	$(2^{k+2}-4)N\log_2(N)+[24S+3\times2^{k+3}+62]N-24S-2^{k+3}-89$	$2N-2$	$3(2^{k+1}-2)N\log_2(N)+(24S+9\times2^{k+1}+31)N-24S-2^{k+3}-45$

where $\|\widetilde{\mathbf{R}}\|_F$ means the Frobenius norm of $\widetilde{\mathbf{R}}$. Since the derivation of the optimal initial values is tedious, we put that in Appendix A. For easy reference, we denote the proposed low-complexity ZF method as the Newton-ZF (N-ZF) method. Finally, we summarize the required complexity for the N-ZF method, the PSE method, and the direct ZF method for a SISO-OFDM system in Table I.

III. PROPOSED ICI CANCELLATION METHOD FOR MIMO-OFDM

ICI suppression is more challenging in MIMO-OFDM systems. In the application of spatial multiplexing, interantenna interference is further introduced. It is possible to formulate the whole system with a linear model and to apply a ZF equalizer to suppress all interference. However, the dimension of the MIMO-OFDM ICI matrix will become much larger than that in a SISO-OFDM system, and the required complexity is even more intractable. In this section, we extend the method proposed in Section II to solve the problem. By considering an $M \times M$ system, where M is the number of transmit/receive antennas, and by using the signal model in SISO-OFDM systems, we can express the frequency-domain signal for the ith receive-antenna as

$$\widetilde{\mathbf{y}}_i = \sum_{j=1}^{M} \widetilde{\mathbf{M}}_{i,j}\widetilde{\mathbf{x}}_j \qquad (11)$$

where $\widetilde{\mathbf{y}}_i$ is the frequency-domain signal in the ith receive antenna, $\widetilde{\mathbf{x}}_j$ is the frequency-domain signal in the jth transmit antenna, and $\widetilde{\mathbf{M}}_{i,j}$ is the ICI matrix for the jth transmit antenna and the ith receive antenna. By stacking all the receive frequency-domain signals from all antennas in a column vector, we have the following signal model:

$$\widetilde{\mathbf{y}} = \widetilde{\mathbf{M}}\widetilde{\mathbf{x}} + \widetilde{\mathbf{z}} \qquad (12)$$

where $\widetilde{\mathbf{y}} = [\widetilde{\mathbf{y}}_1^T, \widetilde{\mathbf{y}}_2^T, \ldots, \widetilde{\mathbf{y}}_M^T]^T$ is the receive frequency-domain signal, $\widetilde{\mathbf{x}} = [\widetilde{\mathbf{x}}_1^T, \widetilde{\mathbf{x}}_2^T, \ldots, \widetilde{\mathbf{x}}_M^T]^T$ is the transmit frequency-domain signal, $\widetilde{\mathbf{z}} = [\widetilde{\mathbf{z}}_1^T, \widetilde{\mathbf{z}}_2^T, \ldots, \widetilde{\mathbf{z}}_M^T]^T$ is the frequency-domain noise, and the frequency-domain ICI channel matrix can be expressed as follows:

$$\widetilde{\mathbf{M}} = \begin{bmatrix} \widetilde{\mathbf{M}}_{1,1} & \widetilde{\mathbf{M}}_{1,2} & \ldots & \widetilde{\mathbf{M}}_{1,M} \\ \widetilde{\mathbf{M}}_{2,1} & \widetilde{\mathbf{M}}_{2,2} & \ldots & \widetilde{\mathbf{M}}_{2,M} \\ \vdots & \vdots & \ddots & \vdots \\ \widetilde{\mathbf{M}}_{M,1} & \widetilde{\mathbf{M}}_{M,2} & \ldots & \widetilde{\mathbf{M}}_{M,M} \end{bmatrix}. \qquad (13)$$

For ease of description, we only consider a 2×2 MIMO-OFDM system in the following derivation. However, the proposed algorithm can be extended to a general $M \times M$ MIMO-OFDM system without any difficulty. Similar to the channel model in SISO-OFDM systems, we also use the LTV model for MIMO-OFDM channels. Thus, we can obtain the MIMO-OFDM ICI matrix given by

$$\widetilde{\mathbf{M}} = \begin{bmatrix} \widetilde{\mathbf{M}}_{1,1} & \widetilde{\mathbf{M}}_{1,2} \\ \widetilde{\mathbf{M}}_{2,1} & \widetilde{\mathbf{M}}_{2,2} \end{bmatrix}$$

$$= \begin{bmatrix} \widetilde{\mathbf{A}}_0 + \mathbf{G}\mathbf{V}_1\mathbf{G}^H\widetilde{\mathbf{A}}_1 & \widetilde{\mathbf{B}}_0 + \mathbf{G}\mathbf{V}_1\mathbf{G}^H\widetilde{\mathbf{B}}_1 \\ \widetilde{\mathbf{C}}_0 + \mathbf{G}\mathbf{V}_1\mathbf{G}^H\widetilde{\mathbf{C}}_1 & \widetilde{\mathbf{D}}_0 + \mathbf{G}\mathbf{V}_1\mathbf{G}^H\widetilde{\mathbf{D}}_1 \end{bmatrix}$$

$$= \begin{bmatrix} \widetilde{\mathbf{A}}_0 & \widetilde{\mathbf{B}}_0 \\ \widetilde{\mathbf{C}}_0 & \widetilde{\mathbf{D}}_0 \end{bmatrix} + \begin{bmatrix} \mathbf{G}\mathbf{V}_1\mathbf{G}^H & \mathbf{0}_N \\ \mathbf{0}_N & \mathbf{G}\mathbf{V}_1\mathbf{G}^H \end{bmatrix} \times \begin{bmatrix} \widetilde{\mathbf{A}}_1 & \widetilde{\mathbf{B}}_1 \\ \widetilde{\mathbf{C}}_1 & \widetilde{\mathbf{D}}_1 \end{bmatrix} \qquad (14)$$

where $\widetilde{\mathbf{A}}_i$, $\widetilde{\mathbf{B}}_i$, $\widetilde{\mathbf{C}}_i$, and $\widetilde{\mathbf{D}}_i$ play the same role as $\widetilde{\mathbf{H}}_i$ in a SISO-OFDM system. The derived signal model is obtained by grouping together subcarrier signals in the same antenna. For the purpose of comparison, we consider a ZF equalization method, ignoring the ICI effect in (14). In this case, the ICI channel matrix turns out to be

$$\widetilde{\mathbf{M}}_s = \begin{bmatrix} \widetilde{\mathbf{A}}_0 & \widetilde{\mathbf{B}}_0 \\ \widetilde{\mathbf{C}}_0 & \widetilde{\mathbf{D}}_0 \end{bmatrix}. \qquad (15)$$

Thus, the equalized signal can be obtained with $\overline{\mathbf{x}}_s = \widetilde{\mathbf{M}}_s^{-1}\widetilde{\mathbf{y}}$. Using the block matrix inversion formula, we know that to obtain the ith subcarrier equalized signal for antenna one or two, the method will require two weights. For ease of reference, we denote this equalization method as a two-tap frequency-domain equalizer (FEQ).

Using the derived MIMO-OFDM ICI matrix in (14), we can now apply Newton's iteration to implement the ZF equalizer. With (6), we can obtain the equalized result as

$$\overline{\mathbf{x}}_k = \sum_{m=0}^{2^k-1} \overline{c}_{k,m}\overline{\mathbf{v}}_m \qquad (16)$$

where $\overline{\mathbf{x}}_k$, $\overline{c}_{k,m}$, and $\overline{\mathbf{v}}_m$ are defined as those in (7). Let the initial matrix $\mathbf{W}_0$ be composed of four $N \times N$ matrices expressed as

$$\mathbf{W}_0 = \begin{bmatrix} \mathbf{W}_\alpha & \mathbf{W}_\beta \\ \mathbf{W}_\gamma & \mathbf{W}_\omega \end{bmatrix} \qquad (17)$$

TABLE II
COMPLEXITY COMPARISON BETWEEN N-ZF AND DIRECT ZF METHODS IN A 2×2 MIMO-OFDM SYSTEM

Methods	Real multiplications	Real divisions	Real additions
Direct ZF	$\frac{32}{3}N^3 + 28N^2 - \frac{2}{3}N$	$4N^2 + 2N$	$\frac{32}{3}N^3 + 22N^2 - \frac{35}{3}N$
N-ZF ($D = 1$)	$(2^{k+3} - 8)N \log_2(N) + (176S + 11 \times 2^{k+3} + \frac{1122}{3})N - 192S - 2^{k+5} - \frac{1020}{3}$	$54N - 20$	$3(2^{k+2} - 4)N \log_2(N) + (176S + 17 \times 2^{k+2} + 322)N - 192S - 2^{k+5} - 316$

and $\overline{\mathbf{v}}_m = [\overline{\mathbf{v}}_{m,1}^T, \overline{\mathbf{v}}_{m,2}^T]^T$. According to the definition of $\overline{\mathbf{v}}_m$, we can obtain $\overline{\mathbf{v}}_{m+1}$ as (18), shown at the bottom of the page. Note that $\widetilde{\mathbf{A}}_i$, $\widetilde{\mathbf{B}}_i$, $\widetilde{\mathbf{C}}_i$, $\widetilde{\mathbf{D}}_i$, and $\mathbf{V}_1$ are all diagonal matrices. It is obvious that if we let $\mathbf{W}_\alpha$, $\mathbf{W}_\beta$, $\mathbf{W}_\gamma$, and $\mathbf{W}_\omega$ be low-bandwidth banded matrices, (18) can be implemented by vector and DFT/IDFT operations. Note that the DFT size is N instead of $2N$. Thus, the required computational complexity is $\mathcal{O}(MN \log_2 N)$. It is straightforward to see that the computational complexity of the direct ZF method is $\mathcal{O}(M^3 N^3)$. The complexity reduction achieved by the proposed method in MIMO-OFDM systems can be greater compared with that in SISO-OFDM systems.

The final problem is how the $2N \times 2N$ initial matrix can be optimally determined. As we did in SISO-OFDM systems, we use the minimum-Frobenius-norm criterion. Since the derivation is lengthy, we put it in Appendix B. Finally, we summarize the computational complexity of the N-ZF and direct ZF methods for a 2×2 MIMO-OFDM system in Table II.

Note that the proposed method can be extended to a general $M_T \times M_R$ MIMO-OFDM system, where $M_T < M_R$. In such a system, we can use the least squares (LS) method, instead of ZF, to cancel ICI. Using the LS method, we can have the equalized signal vector as

$$\overline{\mathbf{x}} = (\widetilde{\mathbf{M}}^H \widetilde{\mathbf{M}})^{-1} \widetilde{\mathbf{M}}^H \widetilde{\mathbf{y}}$$
$$= \widetilde{\mathbf{Q}}^{-1} \overline{\mathbf{y}} \qquad (19)$$

where $\widetilde{\mathbf{Q}} = \widetilde{\mathbf{M}}^H \widetilde{\mathbf{M}}$, and $\overline{\mathbf{y}} = \widetilde{\mathbf{M}}^H \widetilde{\mathbf{y}}$. The matrix $\widetilde{\mathbf{Q}}$, inheriting the properties of $\widetilde{\mathbf{M}}$, consists of diagonal matrices and FFT/IFFT matrices as well. As a result, the proposed method discussed above can be applied. Since the derivation is simple and straightforward, it is omitted here. Due to the application of the LS method, the required complexity in this scenario will be somewhat higher.

IV. PERFORMANCE ANALYSIS

For the proposed algorithm, the iteration number is usually preset. Unlike other iterative algorithms, the convergence is not a concern here. The reason we can use a preset iteration number is due to the fast convergence property of Newton's iteration, as well as our good initial values. If the proposed algorithm converges, only a small number of iterations are necessary. On the other hand, if the proposed algorithm diverges, the preset number of iterations will limit the performance degradation. As a matter of fact, even for divergence cases, we can still have improved SINRs if the iteration number is set properly. We will provide intuitive statements to explain why this is true. It turns out that the determination of the iteration number is simple and straightforward.

Here, we start with the analysis of convergence behavior. After that, we will derive theoretical SINRs that the proposed algorithm can provide. Note that since the SISO/MIMO-OFDM signal models are similar in form, the only difference is the dimension. Thus, we focus on a SISO-OFDM system, but the analysis can be extended to MIMO-OFDM systems. We first perform the eigenvalue decomposition for $\widetilde{\mathbf{R}}_0$ as follows:

$$\widetilde{\mathbf{R}}_0 = \mathbf{U}\mathbf{D}\mathbf{U}^{-1} \qquad (20)$$

where $\mathbf{U} = [\mathbf{u}_0, \mathbf{u}_1, \ldots, \mathbf{u}_{N-1}]$ is a matrix composed of eigenvectors of $\widetilde{\mathbf{R}}_0$, and $\mathbf{D} = \text{diag}([\lambda_0, \lambda_1, \ldots, \lambda_{N-1}]^T)$ consists of eigenvalues λ_i. We assume that $|\lambda_i| \geq |\lambda_j|$ for $i \leq j$. Since $\widetilde{\mathbf{R}}_k = \widetilde{\mathbf{R}}_{k-1}^2$, we can then decompose $\widetilde{\mathbf{R}}_k$ as

$$\widetilde{\mathbf{R}}_k = \mathbf{U}\mathbf{D}^{2^k}\mathbf{U}^{-1}. \qquad (21)$$

If $|\lambda_0| < 1$, then $\widetilde{\mathbf{R}}_k \to \mathbf{0}_N$ as $k \to \infty$. Thus, we can have the convergence condition for Newton's iteration as $\rho(\widetilde{\mathbf{R}}_0) < 1$, where $\rho(\widetilde{\mathbf{R}}_0)$ denotes the spectral radius of $\widetilde{\mathbf{R}}_0$; the spectral radius indicates the largest absolute value of all eigenvalues [34]. This is equivalent to say that for Newton's iteration to converge, the amplitudes of all eigenvalues of $\widetilde{\mathbf{R}}_0$ have to be smaller than one. For a moderate mobile speed, this condition holds for most cases. If not, the number of eigenvalues with amplitudes greater than one is small, and their amplitudes do not deviate from one too much. These results can easily be observed from simulations, though they are difficult to prove theoretically. In what follows, we will first show that even for divergence cases, we may still benefit from Newton's iteration. Let $\mathbf{U}^{-1} = [\mathbf{p}_0, \mathbf{p}_1, \ldots, \mathbf{p}_{N-1}]^T$, $|\lambda_i| > 1$ for $i = 0, 1, \ldots, P - 1$ and $|\lambda_i| < 1$ for $i = P, P + 1, \ldots, N - 1$.

$$\overline{\mathbf{v}}_{m+1} = \begin{bmatrix} \mathbf{W}_\alpha & \mathbf{W}_\beta \\ \mathbf{W}_\gamma & \mathbf{W}_\omega \end{bmatrix} \left\{ \begin{bmatrix} \widetilde{\mathbf{A}}_0 & \widetilde{\mathbf{B}}_0 \\ \widetilde{\mathbf{C}}_0 & \widetilde{\mathbf{D}}_0 \end{bmatrix} + \begin{bmatrix} \mathbf{G}\mathbf{V}_1\mathbf{G}^H & \mathbf{0}_N \\ \mathbf{0}_N & \mathbf{G}\mathbf{V}_1\mathbf{G}^H \end{bmatrix} \begin{bmatrix} \widetilde{\mathbf{A}}_1 & \widetilde{\mathbf{B}}_1 \\ \widetilde{\mathbf{C}}_1 & \widetilde{\mathbf{D}}_1 \end{bmatrix} \right\} \begin{bmatrix} \overline{\mathbf{v}}_{m,1} \\ \overline{\mathbf{v}}_{m,2} \end{bmatrix}$$

$$= \begin{bmatrix} \mathbf{W}_\alpha & \mathbf{W}_\beta \\ \mathbf{W}_\gamma & \mathbf{W}_\omega \end{bmatrix} \left\{ \begin{bmatrix} \widetilde{\mathbf{A}}_0 \overline{\mathbf{v}}_{m,1} + \widetilde{\mathbf{B}}_0 \overline{\mathbf{v}}_{m,2} \\ \widetilde{\mathbf{C}}_0 \overline{\mathbf{v}}_{m,1} + \widetilde{\mathbf{D}}_0 \overline{\mathbf{v}}_{m,2} \end{bmatrix} + \begin{bmatrix} \mathbf{G}\mathbf{V}_1\mathbf{G}^H(\widetilde{\mathbf{A}}_1 \overline{\mathbf{v}}_{m,1} + \widetilde{\mathbf{B}}_1 \overline{\mathbf{v}}_{m,2}) \\ \mathbf{G}\mathbf{V}_1\mathbf{G}^H(\widetilde{\mathbf{C}}_1 \overline{\mathbf{v}}_{m,1} + \widetilde{\mathbf{D}}_1 \overline{\mathbf{v}}_{m,2}) \end{bmatrix} \right\} \qquad (18)$$

By definition, $\widetilde{\mathbf{R}}_k = \mathbf{I}_N - \mathbf{W}_k\widetilde{\mathbf{M}}$. Then, we can represent the ICI matrix as

$$\mathbf{W}_k\widetilde{\mathbf{M}} = \mathbf{I}_N - \sum_{i=0}^{P-1} \lambda_i^{2^k}\mathbf{u}_i\mathbf{p}_i^T - \sum_{j=P}^{N-1} \lambda_j^{2^k}\mathbf{u}_j\mathbf{p}_j^T. \tag{22}$$

As for $\mathbf{W}_k$, we can reformulate it as

$$\mathbf{W}_k = (\mathbf{I}_N + \widetilde{\mathbf{R}}_{k-1})(\mathbf{I}_N + \widetilde{\mathbf{R}}_{k-2})\dots(\mathbf{I}_N + \widetilde{\mathbf{R}}_0)\mathbf{W}_0. \tag{23}$$

By using (21), we can further express $\mathbf{W}_k$ as

$$\mathbf{W}_k = \sum_{j=0}^{N-1} \phi_{j,k}\mathbf{u}_j\mathbf{p}_j^T\mathbf{W}_0 \tag{24}$$

where $\phi_{j,k} = \prod_{i=0}^{k-1}(1 + \lambda_j^{2^i})$. With (22) and (24), the ZF-equalized signal can be expressed as

$$\overline{\mathbf{x}}_k = \widetilde{\mathbf{x}} - \sum_{i=0}^{P-1} \lambda_i^{2^k}\mathbf{u}_i\mathbf{p}_i^T\widetilde{\mathbf{x}} - \sum_{j=P}^{N-1} \lambda_j^{2^k}\mathbf{u}_j\mathbf{p}_j^T\widetilde{\mathbf{x}} + \sum_{j=0}^{N-1} \phi_{j,k}\mathbf{u}_j\mathbf{p}_j^T\widetilde{\mathbf{v}}_0 \tag{25}$$

where $\widetilde{\mathbf{v}}_0 = \mathbf{W}_0\widetilde{\mathbf{v}}$. Since the eigenvectors $\{\mathbf{u}_0, \mathbf{u}_1, \dots, \mathbf{u}_{N-1}\}$ span the N-dimensional space, we can decompose $\widetilde{\mathbf{x}}$ and $\widetilde{\mathbf{v}}_0$ using these eigenvectors. Let $\widetilde{\mathbf{x}} = \sum_{l=0}^{N-1} \beta_l\mathbf{u}_l$ and $\widetilde{\mathbf{v}}_0 = \sum_{l=0}^{N-1} \gamma_l\mathbf{u}_l$, respectively. Then, we can rewrite (25) as

$$\overline{\mathbf{x}}_k = \widetilde{\mathbf{x}} - \sum_{i=0}^{P-1} \lambda_i^{2^k}\beta_i\mathbf{u}_i - \sum_{j=P}^{N-1} \lambda_j^{2^k}\beta_j\mathbf{u}_j + \sum_{j=0}^{N-1} \phi_{j,k}\gamma_j\mathbf{u}_j. \tag{26}$$

Let $\overline{\mathbf{x}}_k = [\overline{x}_{k,0}, \overline{x}_{k,1}, \dots, \overline{x}_{k,N-1}]^T$ and $\widetilde{\mathbf{x}} = [\widetilde{x}_0, \widetilde{x}_1, \dots, \widetilde{x}_{N-1}]^T$. Thus, the mth subcarrier signal after equalization can be expressed as

$$\overline{x}_{k,m} = \widetilde{x}_m + \widetilde{f}_{1,k,m} + \widetilde{f}_{2,k,m} + \widetilde{f}_{3,k,m} \tag{27}$$

where $\widetilde{f}_{1,k,m} = -\sum_{i=0}^{P-1} \lambda_i^{2^k}\beta_i\mathbf{u}_i(m)$, $\widetilde{f}_{2,k,m} = -\sum_{j=P}^{N-1} \lambda_j^{2^k}\beta_j\mathbf{u}_j(m)$, and $\widetilde{f}_{3,k,m} = \sum_{j=0}^{N-1} \phi_{j,k}\gamma_j\mathbf{u}_j(m)$. From (27), we can see that the equalized signal suffers from three interference terms. For $\widetilde{f}_{1,k,m}$, it will become large when k increases; however, for $\widetilde{f}_{2,k,m}$, it will become small when k increases.

As for the noise term $\widetilde{f}_{3,k,m}$, its dependence on k is not strong. As mentioned, only a few eigenvalues' amplitudes will be larger than one (i.e., P is small), and their amplitudes often do not deviate from one too much. Then, it is easy to see that the decreasing amount of $\widetilde{f}_{2,k,m}$ will be larger than the increasing amount of $\widetilde{f}_{1,k,m}$ in the early iteration. Thus, for divergence cases, the interference will decrease first and then increase as the iteration proceeds. If we can stop the iteration before the overall interference increases, we can still have performance gain even though the iteration diverges eventually. Additionally, we can increase D to make the initial matrix closer to the exact matrix inverse. This way, P may be minimized, and $\widetilde{f}_{1,k,m}$ will decrease, which makes the proposed method work better. Because of the fast convergence property of Newton's method, the

number of iterations required is small. For example, it can be as small as one or two when $D = 1$. For divergent cases, the overall interference still decreases in the first one or two iterations.

Since the performance of an OFDM-based system depends on each subcarrier SINR, we will analyze the subcarrier SINR of the proposed algorithm in the sequel. From (3), we can express the equalized signal as $\mathbf{W}_k\widetilde{\mathbf{y}} = \mathbf{T}_k\widetilde{\mathbf{x}} + \mathbf{W}_k\widetilde{\mathbf{z}}$, where $\mathbf{T}_k = \sum_{m=0}^{2^k-1} \overline{c}_{k,m}(\mathbf{W}_0\widetilde{\mathbf{M}})^{m+1}$ is the equalized ICI matrix. Ideally, $\mathbf{T}_k$ will be an identity matrix. Let $\widetilde{\mathbf{z}} = [\widetilde{z}_0, \widetilde{z}_1, \dots, \widetilde{z}_{N-1}]^T$, $\sigma_{\widetilde{x}}^2 = E\{|\widetilde{x}_i|^2\}$, $\sigma_{\widetilde{z}}^2 = E\{|\widetilde{z}_i|^2\}$ $(0 \le i \le N-1)$, and $\psi = (\sigma_{\widetilde{z}}^2/\sigma_{\widetilde{x}}^2)$. The subcarrier SINR for the proposed method with k iterations in the ith subcarrier, which is denoted as SINR$_{k,i}$, can be shown as

$$\text{SINR}_{k,i} = \frac{E\left\{\left|t_{i,i}^k\widetilde{x}_i\right|^2\right\}}{E\left\{\left|\sum_{\substack{j=0\\j\neq i}}^{N-1} t_{i,j}^k\widetilde{x}_j\right|^2\right\} + E\left\{\left|\sum_{j=0}^{N-1} w_{i,j}^k\widetilde{z}_j\right|^2\right\}}$$

$$= \frac{\left|t_{i,i}^k\right|^2}{\sum_{\substack{j=0\\j\neq i}}^{N-1}\left|t_{i,j}^k\right|^2 + \psi\sum_{j=0}^{N-1}\left|w_{i,j}^k\right|^2} \tag{28}$$

where $t_{i,j}^k = \mathbf{T}_k(i,j)$, and $w_{i,j}^k = \mathbf{W}_k(i,j)$. For comparison, we also calculate the SINR in the ith subcarrier before equalization, which is denoted as SINR$_i$, as

$$\text{SINR}_i = \frac{E\left\{|\widetilde{m}_{i,i}\widetilde{x}_i|^2\right\}}{E\left\{\left|\sum_{\substack{j=0\\j\neq i}}^{N-1}\widetilde{m}_{i,j}\widetilde{x}_j\right|^2\right\} + E\{|\widetilde{z}_i|^2\}}$$

$$= \frac{|\widetilde{m}_{i,i}|^2}{\sum_{\substack{j=0\\j\neq i}}^{N-1}|\widetilde{m}_{i,j}|^2 + \psi}. \tag{29}$$

As a result, we must calculate each element in $\mathbf{T}_k$ and $\mathbf{W}_k$ for SINR$_{k,i}$. To make the following derivation more compact, we rewrite the ICI matrix as $\widetilde{\mathbf{M}} = \sum_{r=0}^{R}\widetilde{\mathbf{V}}_r\widetilde{\mathbf{H}}_r$, where $\widetilde{\mathbf{V}}_0 = \mathbf{I}_N$, and $R = 1$. Since $\widetilde{\mathbf{M}} = \sum_{r=0}^{R}\widetilde{\mathbf{V}}_r\widetilde{\mathbf{H}}_r$, the equalized ICI matrix $\mathbf{T}_k$ can be expanded as (30), shown at the bottom of the next page, where $\overline{\mathbf{A}}_m = \prod_{f=0}^{m}\mathbf{W}_0\widehat{\mathbf{V}}_{r_{m,f}}\widehat{\mathbf{H}}_{r_{m,f}}$, and $\overline{\mathbf{A}}_{-1} = \mathbf{I}_N$. Using the same way, we also expand $\mathbf{W}_k$ as

$$\mathbf{W}_k = \sum_{m=0}^{2^k-1}\overline{c}_{k,m}\left\{\sum_{r_{m,0}=0}^{R}\sum_{r_{m,1}=0}^{R}\dots\sum_{r_{m,m-1}=0}^{R}\overline{\mathbf{B}}_m\right\} \tag{31}$$

where $\overline{\mathbf{B}}_m = \overline{\mathbf{A}}_{m-1}\mathbf{W}_0$. We then calculate each element $\overline{\mathbf{A}}_m(i_m, j_m)$. For brevity of presentation, we consider the case of $D = 0$. To compact and simplify the notation, we redefine $\widetilde{\mathbf{h}}_r = [\widetilde{h}_0^r, \widetilde{h}_1^r, \dots, \widetilde{h}_{N-1}^r]^T$ and $\widetilde{\mathbf{v}}_r = [\widetilde{v}_0^r, \widetilde{v}_1^r, \dots, \widetilde{v}_{N-1}^r]^T$, and we let $w_i = w_{i,i}$. Since $\widetilde{\mathbf{V}}_{r_{m,f}}$ is a circulant matrix, it can be expressed as $\widetilde{\mathbf{V}}_{r_{m,f}} = [cir(\widetilde{\mathbf{v}}_{r_{m,f}})]^T$. Furthermore, from the definition, we have $\widetilde{\mathbf{H}}_{r_{m,f}} = \text{diag}(\widetilde{\mathbf{h}}_{r_{m,f}})$. For $m = 0$, we have $\overline{\mathbf{A}}_0(i_0, j_0)$ as

$$\overline{\mathbf{A}}_0(i_0, j_0) = w_{i_0}\widetilde{v}_{\langle j_0-i_0, N\rangle}^{r_{0,0}}\widetilde{h}_{j_0}^{r_{0,0}}. \tag{32}$$

Then, we can obtain $\bar{\mathbf{A}}_1 = (\mathbf{W}_0 \widetilde{\mathbf{V}}_{r_{1,1}} \widetilde{\mathbf{H}}_{r_{1,1}}) \bar{\mathbf{A}}_0$ and $\bar{\mathbf{A}}_2 = (\mathbf{W}_0 \widetilde{\mathbf{V}}_{r_{2,2}} \widetilde{\mathbf{H}}_{r_{2,2}}) \bar{\mathbf{A}}_1$ accordingly. By repeating this process, we can obtain a formula for $m \geq 1$. For $m \geq 1$, we have $\bar{\mathbf{A}}_m(i_m, j_m)$, as in (33), shown at the bottom of the page. With $\widetilde{\mathbf{M}} = \sum_{r=0}^{R} \widetilde{\mathbf{V}}_r \widetilde{\mathbf{H}}_r$, we can expand $\widetilde{m}_{i,j}$ as

$$\widetilde{m}_{i,j} = \sum_{r=0}^{R} \widetilde{v}^r_{\langle j-i, N \rangle} \widetilde{h}^r_j. \tag{34}$$

From (57) and (34), we can express w_i as

$$w_i \approx \frac{\left(\sum_{r=0}^{R} \widetilde{v}^r_0 \widetilde{h}^r_i \right)^*}{\sum_{j \in \Omega'} | \sum_{r=0}^{R} \widetilde{v}^r_{\langle j-i, N \rangle} \widetilde{h}^r_j |^2}. \tag{35}$$

Since we have derived $\widetilde{v}^j_i$ and $\widetilde{h}^j_i$, we can then calculate w_i. Thus, we can have $\bar{\mathbf{A}}_m(i_m, j_m)$. By using (30) and $\bar{\mathbf{A}}_m(i_m, j_m)$, we can obtain $\mathbf{T}_k$. By using the relation of $\bar{\mathbf{B}}_m = \bar{\mathbf{A}}_{m-1} \mathbf{W}_0$, (33), and (35), we can compute $\bar{\mathbf{B}}_m(i_m, j_m)$ as

$$\bar{\mathbf{B}}_m(i_m, j_m) = \frac{\bar{\mathbf{A}}_{m-1}(i_m, j_m) \left(\sum_{r=0}^{R} \widetilde{v}^r_0 \widetilde{h}^r_{j_m} \right)^*}{\sum_{j \in \Omega''} \left| \sum_{r=0}^{R} \widetilde{v}^r_{\langle j-j_m, N \rangle} \widetilde{h}^r_j \right|^2} \tag{36}$$

where $\Omega'' = \langle j_m - S : j_m + S, N \rangle$. From (31) and (36), we can then calculate $\mathbf{W}_k$. Having $\mathbf{T}_k$ and $\mathbf{W}_k$ ready, we can finally evaluate $\mathrm{SINR}_{k,i}$ in (28). With (34), we can further express SINR_i in (29) as

$$\mathrm{SINR}_i = \frac{\left| \sum_{r=0}^{R} \widetilde{v}^r_0 \widetilde{h}^r_i \right|^2}{\sum_{\substack{j=0 \\ j \neq i}}^{N-1} \left| \sum_{r=0}^{R} \widetilde{v}^r_{\langle j-i, N \rangle} \widetilde{h}^r_j \right|^2 + \psi}. \tag{37}$$

As for the case of $D \neq 0$, it can be derived the same way.

V. SIMULATION RESULTS

In this section, we report simulations to demonstrate the effectiveness of the proposed method. We consider OFDM systems with $N = 128$ and the CP size of 16. The modulation scheme is 16-quadrature amplitude modulation (16-QAM). The channel length is set to $L = 15$, and the power delay profile is characterized by an exponential function, i.e., $\sigma_l^2 = e^{-l/L} / \sum_{i=0}^{L-1} e^{-i/L}$, where l is the tap index. Each channel tap is generated by Jakes' model [41]. Here, we assume that the channel response is exactly known for the direct ZF method. For the proposed method, the parameters of the LTV channel model are obtained by LS fittings. Define the normalized Doppler frequency as $f_d = f_d N T_s$, where f_d is the maximum Doppler frequency, and T_s is the sampling period. For a MIMO-OFDM system, its settings are the same as those in a SISO-OFDM system. Specifically, we consider a 2×2 MIMO-OFDM system. Since the N-ZF method with $S = 2$ have the similar performance to that with $S = N/2 - 1$, we set $S = 2$ for all simulations.

First, we evaluate the validity of the analytic output SINRs for the proposed method. Two cases are considered: case 1 meets the convergence condition derived in Section IV, whereas case 2 does not. We consider a SISO-OFDM system, and let $f_d = 0.1$, signal-to-noise ratio (SNR) = 35 dB, $S = 2$, and $D = 0$. Fig. 1 shows the analytic subcarrier SINRs for case 1. Since the simulated SINRs are almost identical to the analytic SINRs, they are not shown in the figure. In this figure, we find that each subcarrier exhibits a different SINR due to the characteristic of the frequency-selective channel. In addition, subcarrier SINRs are all increased as the number of iterations is increased. The performance of the proposed method with two iterations is similar to that with three iterations. We can also find that the output SINRs of the proposed method are very close to those of the direct ZF method. Fig. 2 shows analytic subcarrier SINRs for case 2. We see that even in this divergence case,

$$\mathbf{T}_k = \sum_{m=0}^{2^k-1} \bar{c}_{k,m} \left\{ \sum_{r_{m,0}=1}^{R} \mathbf{W}_0 \widetilde{\mathbf{V}}_{r_{m,0}} \widetilde{\mathbf{H}}_{r_{m,0}} \sum_{r_{m,1}=1}^{R} \mathbf{W}_0 \widetilde{\mathbf{V}}_{r_{m,1}} \widetilde{\mathbf{H}}_{r_{m,1}} \cdots \sum_{r_{m,m}=1}^{R} \mathbf{W}_0 \widetilde{\mathbf{V}}_{r_{m,m}} \widetilde{\mathbf{H}}_{r_{m,m}} \right\}$$

$$= \sum_{m=0}^{2^k-1} \bar{c}_{k,m} \left\{ \sum_{r_{m,0}=0}^{R} \sum_{r_{m,1}=0}^{R} \cdots \sum_{r_{m,m}=0}^{R} \prod_{f=0}^{m} \mathbf{W}_0 \widetilde{\mathbf{V}}_{r_{m,f}} \widetilde{\mathbf{H}}_{r_{m,f}} \right\}$$

$$= \sum_{m=0}^{2^k-1} \bar{c}_{k,m} \left\{ \sum_{r_{m,0}=0}^{R} \sum_{r_{m,1}=0}^{R} \cdots \sum_{r_{m,m}=0}^{R} \bar{\mathbf{A}}_m \right\} \tag{30}$$

$$\bar{\mathbf{A}}_m(i_m, j_m) = \sum_{k_{m-1}=0}^{N-1} \sum_{k_{m-2}=0}^{N-1}, \ldots, \sum_{k_0=0}^{N-1} w_{k_0} w_{k_1}, \ldots, w_{k_{m-1}} w_{i_m} \widetilde{v}^{r_{m,m}}_{\langle j_m - k_{m-1}, N \rangle}$$

$$\widetilde{v}^{r_{m,m-1}}_{\langle k_{m-1} - k_{m-2}, N \rangle}, \ldots, \widetilde{v}^{r_{m,1}}_{\langle k_1 - k_0, N \rangle} \widetilde{v}^{r_{m,0}}_{\langle k_0 - i_m, N \rangle} \widetilde{h}^{r_{m,m}}_{j_m} \widetilde{h}^{r_{m,m-1}}_{k_{m-1}}, \ldots, \widetilde{h}^{r_{m,0}}_{k_0} \tag{33}$$
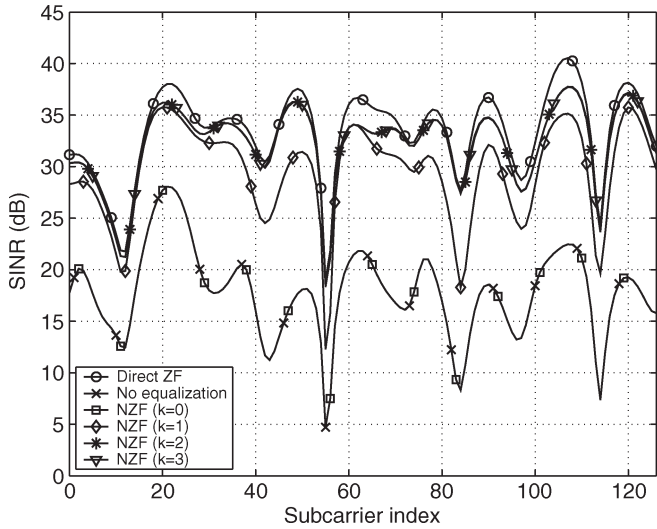
Fig. 1. SINR analysis of the N-ZF method ($D = 0$ and $S = 2$) for case 1, where $f_d = 0.1$, and SNR = 35 dB.

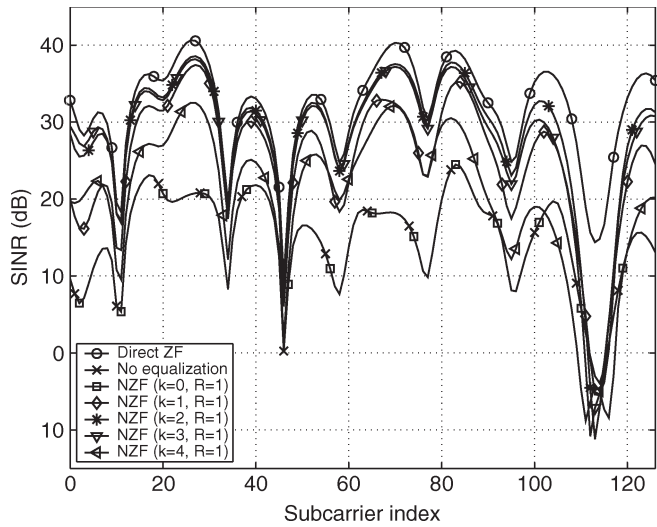Fig. 2. SINR analysis of the N-ZF method ($D = 0$ and $S = 2$) for case 2, where $f_d = 0.1$, and SNR = 35 dB.
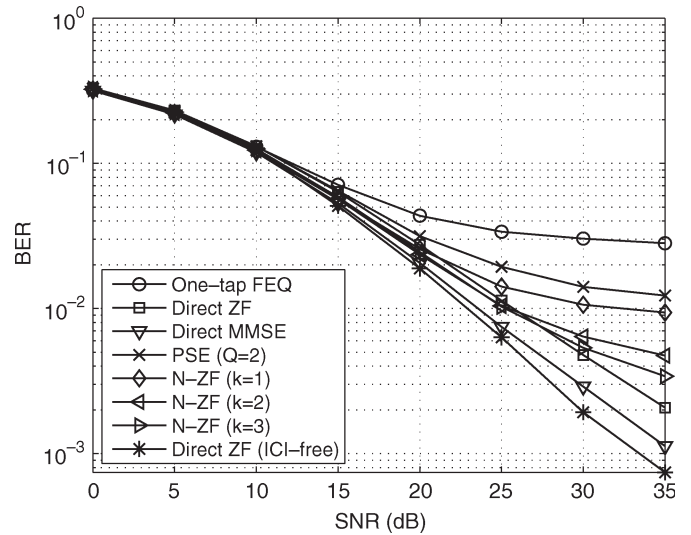

Fig. 3. BER comparison among one-tap FEQ, PSE, N-ZF ($D = 0$ and $S = 2$), direct ZF, and direct MMSE methods in a SISO-OFDM system; $f_d = 0.1$, and 16-QAM.
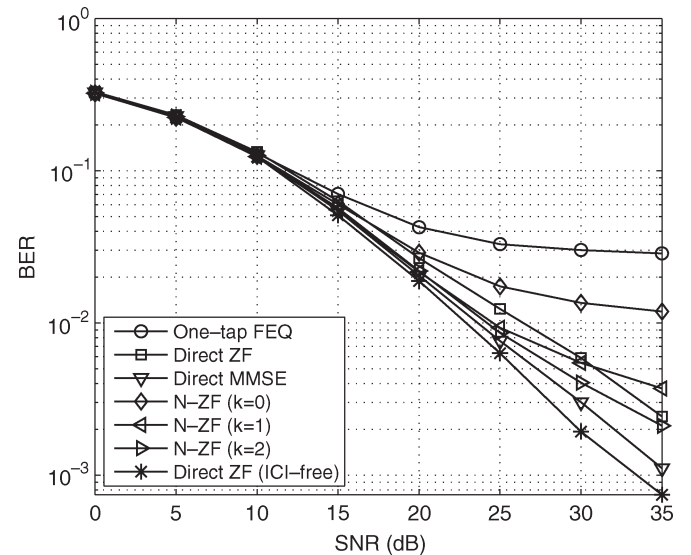

Fig. 4. BER comparison among one-tap FEQ, N-ZF ($D = 1$ and $S = 2$), direct ZF, and direct MMSE methods in an SISO-OFDM system; $f_d = 0.1$, and 16-QAM.

SINRs are still increased for the first two or three iterations. For the fourth iteration, subcarrier SINRs start to fall. The result for $D = 1$ is similar to that for $D = 0$, except that the required number of iterations is reduced to one or two.

Next, we consider the performance comparison for the proposed and conventional methods in a SISO-OFDM system. Here, f_d is set to 0.1. Specifically, the bit error rate (BER) is used as the performance measure. For the benchmarking purpose, we also show the result of the direct MMSE method and that of the direct ZF method with $f_d = 0$ (ICI-free). From extensive simulations, we also find that the performance of the PSE method cannot be further enhanced when $Q > 2$. For this reason, we only show the result for $Q = 2$. Fig. 3 shows the BER performance comparison for $D = 0$. As we can see, the performance of the PSE method is limited and has an error floor phenomenon. The N-ZF method outperforms the PSE method, even with one iteration only. As mentioned, there is a convergence condition for the PSE method. This condition is

totally dependent on the channel. The N-ZF method also has its convergence condition. However, it depends on the initial matrix as well as the channel. It is then possible to reduce the probability of divergence through the determination of $\mathbf{W}_0$. This is the main reason the N-ZF method can outperform the PSE method. The required complexity of the N-ZF method is lower than that of the PSE method (this can be seen later). Moreover, the performance of the N-ZF method with three iterations can approach that of the direct ZF method. Here, the performance of the direct ZF is only slightly worse than that of the direct MMSE method. Fig. 4 shows the BER performance comparison for $D = 1$. It is obvious that the N-ZF method can quickly approach the direct ZF method with one or two iterations. Note that the N-ZF method with two iterations can even perform slightly better than the direct ZF method. This behavior is interesting and can be explained as follows.
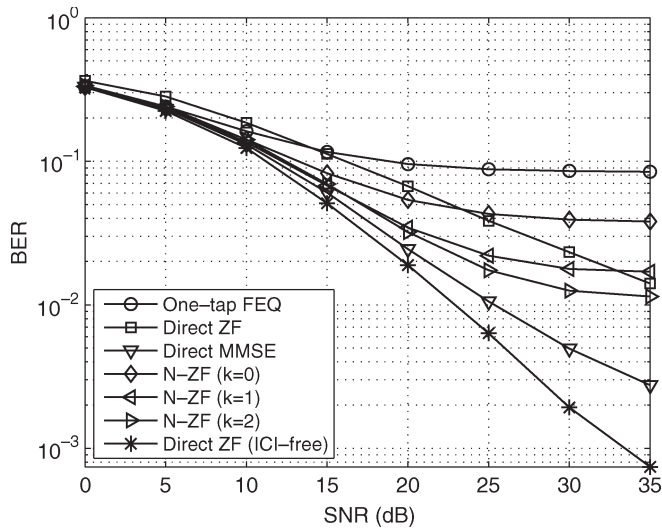
Fig. 5. BER comparison among one-tap FEQ, N-ZF ($D = 1$ and $S = 2$), direct ZF, and direct MMSE methods in an SISO-OFDM system; $f_d = 0.2$, and 16-QAM.
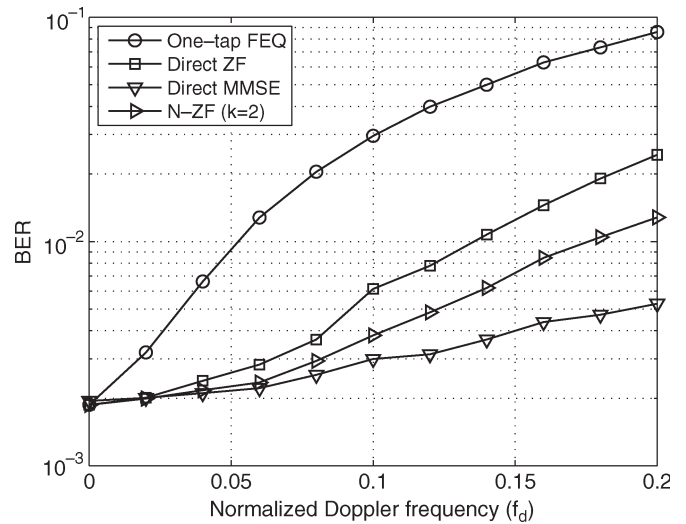

Fig. 6. BER comparison among one-tap FEQ, N-ZF ($D = 1$ and $S = 2$), direct ZF, and direct MMSE methods in an SISO-OFDM system; $f_d = 0 \sim 0.2$, 16-QAM, and SNR = 30 dB.

The N-ZF method only iterates Newton's method two or three times, and it may not converge completely in all cases. As known, the direct ZF method has a noise enhancement problem. It is then possible that the noise enhancement caused by the N-ZF method is smaller. As a result, the performance of the N-ZF method can be better than that of the direct ZF method. If the convergence condition is met and the number of iterations is high enough, the performance of the N-ZF and direct ZF methods will be the same. This phenomenon has been verified by simulations, but the result is not shown here. Compared with Fig. 3, we see that the N-ZF method with $D = 1$ has better performance than that with $D = 0$, and it can approach the direct ZF method more quickly.

To test the limitation of all algorithms, we consider a more severe case in which $f_d = 0.2$. Fig. 5 shows the simulation result. In this figure, we see that the N-ZF method can still work, but its performance is degraded since ICI is much larger than that in the previous cases. In addition, we can see that the degradation of the MMSE method is smaller and that the performance gap between the ZF and MMSE methods become larger. We also conduct simulations to evaluate the robustness of all algorithms to the variation of the normalized Doppler frequency. Fig. 6 shows the results for f_d, varying from 0 to 0.2. Here, the SNR is set to 30 dB. In this figure, we can see that the performance of all methods is degraded as the normalized Doppler frequency is increased. Furthermore, the MMSE method is the most robust method, followed by the N-ZF method.

Table III summarizes the required computational complexity of the direct ZF method, the PSE method, and the N-ZF method for the simulation setting shown above. In this table, the ratios inside parentheses indicate the number of operations required for the N-ZF method divided by those for the direct ZF and PSE methods. The first ratio is for the direct ZF method, and the second ratio is for the PSE method. From the above simulations, we can say that for $D = 0$, the required iteration number for the N-ZF method is two or three, whereas for $D = 1$, it is one or two. In Table III, we can see that the N-ZF method with $D = 0$

can save tremendous computations compared to the direct ZF method. With two (three) iterations, its multiplication complexity is only 0.007 (0.015) of that of the direct ZF method. As for the case of $D = 1$, it also saves a lot of computations compared to the direct ZF method. We can find that the multiplication complexity of the N-ZF method with one iteration (two iterations) is only 0.008 (0.013) of that of the direct ZF method. As to additions, the complexity ratios are similar to those of multiplications. As to divisions, the ratios are 0.016 and 0.015 for $D = 0$ and $D = 1$, respectively. Compared to the PSE method ($Q = 2$), the N-ZF method ($k = 1$ and $D = 0$) also has lower complexity and better performance. Its required multiplications (additions/divisions) is 0.85 (0.745/0.5) of those of the PSE method.

Finally, we report the simulation results for a 2×2 MIMO-OFDM system. From previous simulations, we can see that the computational complexity of the N-ZF method with $D = 0$ and $D = 1$ is similar when the required number of iterations is taken into account. However, the N-ZF method with $D = 1$ tends to have better results. Thus, we will only consider the N-ZF method with $D = 1$. Here, we consider two environments, i.e., $f_d = 0.05$ and 0.1. Fig. 7 depicts the BER performance for the proposed method, the direct ZF method, and the direct MMSE method for $f_d = 0.05$. In this figure, we see that the two-tap FEQ method has an irreducible error floor due to ICI. It is obvious that the N-ZF method can effectively suppress the ICI and that its performance can quickly approach that of the direct ZF method. As we can see, the iteration number can be as small as one. In addition, note that the direct MMSE method does not give too much performance enhancement compared with the direct ZF method. Fig. 8 illustrates the BER performance for the case of $f_d = 0.1$. The N-ZF method can still effectively suppress the interference, and its performance can approach that of the direct ZF method quickly. In this case, one or two iterations are sufficient for the N-ZF method. Note further that with two iterations, the N-ZF method can outperform the direct ZF method. Table IV summarizes the required computational complexity of the direct

TABLE III
COMPLEXITY COMPARISON AMONG N-ZF, PSE, AND DIRECT ZF METHODS IN AN SISO-OFDM SYSTEM ($N = 128$ AND $S = 2$)

| Methods	Real multiplications (ratio)	Real divisions (ratio)	Real additions (ratio)
Direct ZF	2910848	16512	2885824
PSE ($Q = 2$)	10240	512	12544
N-ZF ($D = 0, k = 1$)	8704 (0.003, 0.85)	256 (0.016, 0.5)	9344 (0.003, 0.745)
N-ZF ($D = 0, k = 2$)	19968 (0.007, 1.95)	256 (0.016, 0.5)	22656 (0.008, 1.806)
N-ZF ($D = 0, k = 3$)	42496 (0.015, 4.15)	256 (0.016, 0.5)	49280 (0.017, 3.929)
N-ZF ($D = 1, k = 0$)	17007 (0.006, 1.661)	254 (0.015, 0.496)	12315 (0.004, 0.982)
N-ZF ($D = 1, k = 1$)	23655 (0.008, 2.310)	254 (0.015, 0.496)	19987 (0.007, 1.593)
N-ZF ($D = 1, k = 2$)	36951 (0.013, 3.609)	254 (0.015, 0.496)	35331 (0.012, 2.817)
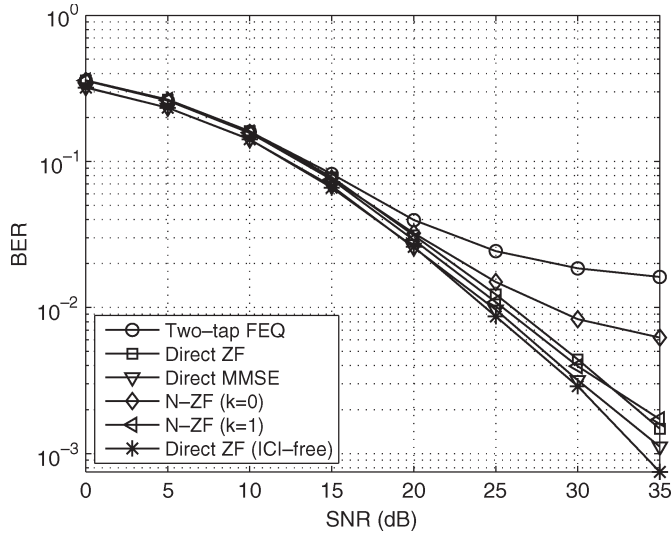
Fig. 7. BER comparison among two-tap FEQ, N-ZF ($D = 1$ and $S = 2$), direct ZF, and direct MMSE methods in a 2×2 MIMO-OFDM system; $f_d = 0.05$, and 16-QAM.
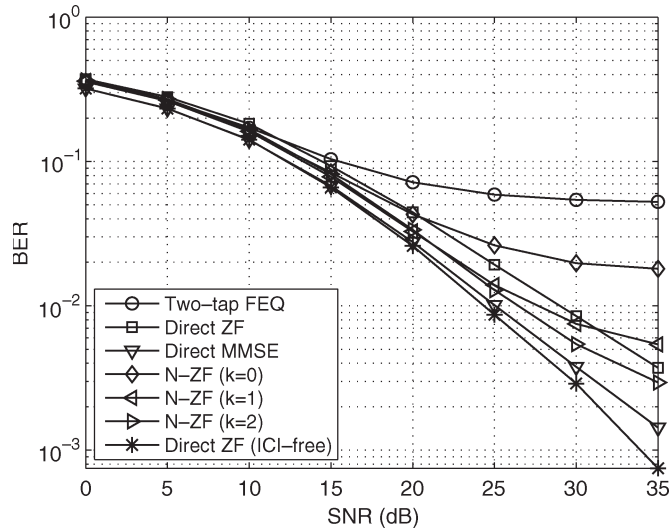

Fig. 8. BER comparison among two-tap FEQ, N-ZF ($D = 1$ and $S = 2$), direct ZF, and direct MMSE methods in a 2×2 MIMO-OFDM system; $f_d = 0.1$, and 16-QAM.

ZF and N-ZF methods. With one iteration, the multiplication (addition) complexity of the N-ZF method ($k = 1$) is only 0.0053 (0.005) of that of the direct ZF method. With two iterations, the complexity ratios of multiplications and additions is 0.0069 and 0.0067.

TABLE IV
COMPLEXITY COMPARISON BETWEEN N-ZF AND DIRECT ZF METHODS IN A 2×2 MIMO-OFDM SYSTEM ($N = 128$ AND $S = 2$)

Methods	Real multiplications (ratio)	Real divisions (ratio)	Real additions (ratio)
Direct ZF	22828288	65792	22728576
N-ZF ($D = 1$, $k = 0$)	103436 (0.0045)	6892 (0.1048)	94244 (0.0041)
N-ZF ($D = 1$, $k = 1$)	121836 (0.0053)	6892 (0.1048)	113668 (0.0050)
N-ZF ($D = 1$, $k = 2$)	158636 (0.0069)	6892 (0.1048)	152516 (0.0067)

Comparing SISO-OFDM and MIMO-OFDM systems, we find that the reduction in computational complexity is greater in a MIMO-OFDM system than that in a SISO-OFDM system. In a SISO-OFDM system, the ratio of multiplications is 0.013, while that in a MIMO-OFDM system is 0.0069 ($D = 1$ and $k = 2$). This is because the complexity of the direct ZF method is proportional to $\mathcal{O}(M^3 N^3)$, whereas that of the N-ZF method is proportional to $\mathcal{O}(MN \log_2 N)$. As a result, we can save more computations as M increases. In addition, when N gets larger, the reduction in computations becomes more apparent as well.

Another important property of the proposed N-ZF method is that it can trade the desired performance for the required complexity. However, the direct ZF method does not have such a choice. This property will make the N-ZF method a more efficient method since it can adapt itself to various SNR environments. If the operated SNR is not high, the iteration number can be reduced. For example, in Fig. 3, it only requires one iteration to approach the direct ZF method when SNR is less than 25 dB.

VI. CONCLUSION

In high-mobility environments, the quasi-static channel assumption for SISO/MIMO-OFDM systems no longer holds, and ICI tends to become the performance bottleneck. The direct ZF equalization method, relying on the inversion of the ICI matrix, may require very high computational complexity. In this paper, we have proposed a low-complexity ZF algorithm to solve the problem. By exploring the structure inherent in the ICI matrix, we develop a method that employs Newton's
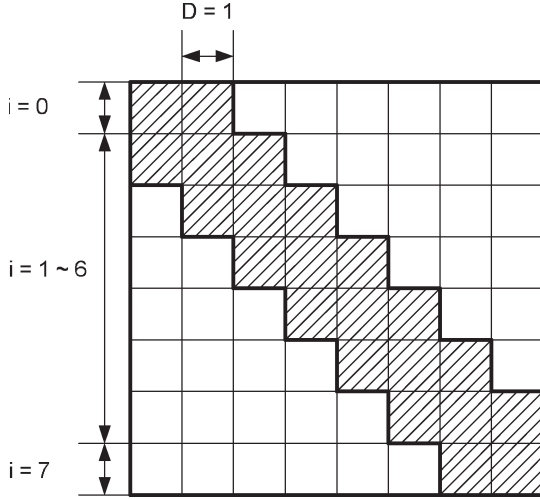
Fig. 9. Example of the structure of a banded initial matrix for $N = 8$ and $D = 1$. The elements in the shaded area are nonzeros, while the others are zeros.

Fig. 10. Example of $\mathbf{A}_i$ for $N = 8$ and $D = 1$. Note that $\mathbf{A}_i$ overlaps with $\mathbf{A}_{i-1}$ and $\mathbf{A}_{i+1}$.

iteration for the matrix inversion. By using our formulation, we effectively use FFTs/IFFTs in the iterative process. Simulations show that while the proposed algorithm can have comparable performance with the direct ZF method, its computational complexity is much lower. We also analyze the convergence behavior of the proposed algorithm and derive the theoretical output SINRs. Note that FFT/IFFT operations are available in an OFDM-based transceiver. Thus, the proposed algorithm only requires limited extra circuits, and the implementation complexity of the proposed method can be lower, facilitating its real-world applications. With the similar idea, it is possible to derive a low-complexity MMSE equalization method that employs Newton's iteration. In some scenarios, the MMSE method can significantly outperform the ZF method. Investigation in this topic is now underway.

APPENDIX A
DERIVATION OF THE INITIAL VALUE FOR SISO-OFDM SYSTEMS

Let $\mathbf{W}$ be a banded matrix with bandwidth D. Then, the minimum-Frobenius-norm criterion is given by

$$\mathbf{W}_0 = \arg \min_{\mathbf{w}} \|\mathbf{I}_N - \mathbf{W}\widetilde{\mathbf{M}}\|_F^2. \qquad (38)$$

Before the derivation of the optimal solution in (38), we first observe a property in a banded matrix. Fig. 9 shows an example of a banded initial matrix for $N = 8$ and $D = 1$. In the figure, only the data in the shaded area are nonzeros. Note that the number of the nonzero elements in each row may not be the same. For the zeroth and seventh rows, the number of the nonzero elements is two. For the rest of rows, the number of the nonzero elements is three. For a general case, the number of the nonzero elements in the ith row first increases, remains the same, and finally decreases (as i increases). Due to this property, we need to consider the three cases when solving (38). Define $\widetilde{m}_{i,j} = \widetilde{\mathbf{M}}(i,j)$, $w_{i,j} = \mathbf{W}_0(i,j)$, and $a_{i,j} = \sum_{n=0}^{N-1} \widetilde{m}_{i,n}^* \widetilde{m}_{j,n}$. By differentiating (38) with respect to
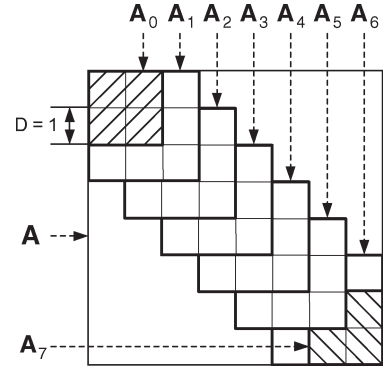
$w_{i,j}^*$ and setting the result to zero, we can obtain the following equation:

$$\mathbf{A}_i \mathbf{w}_i = \mathbf{m}_i, \qquad i = 0, 1, \dots, N-1 \qquad (39)$$

where $\mathbf{w}_i$ is the ith row of the optimum $\mathbf{W}_0$. $\mathbf{A}_i$, $\mathbf{w}_i$, and $\mathbf{m}_i$ for the aforementioned three cases are defined as follows.

1) For $i = D, D+1, \dots, N-1-D$, we have

$$\mathbf{A}_i = \begin{bmatrix} a_{i-D,i-D} & \cdots & a_{i-D,i+D} \\ \vdots & \ddots & \vdots \\ a_{i+D,i-D} & \cdots & a_{i+D,i+D} \end{bmatrix} \qquad (40)$$

$$\mathbf{w}_i = [w_{i,i-D}, w_{i,i-D+1}, \dots, w_{i,i+D}]^T \qquad (41)$$

$$\mathbf{m}_i = [\widetilde{m}_{i-D,i}^*, \widetilde{m}_{i-D+1,i}^*, \dots, \widetilde{m}_{i+D,i}^*]^T. \qquad (42)$$

2) For $i = 0, 1, \dots, D-1$, we have

$$\mathbf{A}_i = \mathbf{A}_D(0 : D+i, 0 : D+i) \qquad (43)$$

$$\mathbf{w}_i = [w_{i,0}, w_{i,1}, \dots, w_{i,i+D}]^T \qquad (44)$$

$$\mathbf{m}_i = [\widetilde{m}_{0,i}^*, \widetilde{m}_{1,i}^*, \dots, \widetilde{m}_{i+D,i}^*]^T \qquad (45)$$

where $\mathbf{C}(i_1 : i_2, j_1 : j_2)$ indicates a submatrix of $\mathbf{C}$, obtained from the i_1th row to the i_2th row and from the j_1th column to the j_2th column of $\mathbf{C}$.

3) For $i = N-D, N-D+1, \dots, N-1$, we have

$$\mathbf{A}_i = \mathbf{A}_{N-1-D}(i-N+1+D : 2D, i-N+1+D : 2D) \qquad (46)$$

$$\mathbf{w}_i = [w_{i,i-D}, w_{i,i-D+1}, \dots, w_{i,N-1}]^T \qquad (47)$$

$$\mathbf{m}_i = [\widetilde{m}_{i-D,i}^*, \widetilde{m}_{i-D+1,i}^*, \dots, \widetilde{m}_{N-1,i}^*]^T. \qquad (48)$$

Note that $\mathbf{A}_i$ in the second case is an upper left submatrix of $\mathbf{A}_D$ in (40), while that in the third case is a lower right submatrix of $\mathbf{A}_{N-1-D}$ in (40). Now, we can obtain the optimum solution for (38) by $\mathbf{w}_i = \mathbf{A}_i^{-1}\mathbf{m}_i$. To clearly understand the structure of $\mathbf{A}_i$, we show an example in Fig. 10 ($N = 8$ and $D = 1$). In this figure, we can see that $\mathbf{A}_0$ is the upper left 2×2 submatrix of $\mathbf{A}_1$. For $i = 1, 2, \dots, 5$, the lower right 2×2 submatrix of $\mathbf{A}_i$ is exactly the same as the upper left 2×2 submatrix of $\mathbf{A}_{i+1}$. The lower right 2×2 submatrix of $\mathbf{A}_6$ is $\mathbf{A}_7$. By using this property, we can obtain a recursive algorithm for fast computation of $\mathbf{A}_i^{-1}$.

Since $a_{j,i} = a_{i,j}^*$, $\mathbf{A}_i$ is a Hermitian matrix. For $i = D, D + 1, \ldots, N - 2 - D$, we can further partition $\mathbf{A}_i$ into the following form:

$$\mathbf{A}_i = \begin{bmatrix} s_i & \mathbf{s}_i^H \\ \mathbf{s}_i & \mathbf{U}_i \end{bmatrix} \tag{49}$$

and $\mathbf{A}_{i+1}$ into the following form:

$$\mathbf{A}_{i+1} = \begin{bmatrix} \mathbf{U}_i & \widetilde{\mathbf{u}}_{i+1} \\ \widetilde{\mathbf{u}}_{i+1}^H & \widetilde{u}_{i+1} \end{bmatrix} \tag{50}$$

where s_i and $\widetilde{u}_{i+1}$ are scalars, $\mathbf{s}_i$ and $\widetilde{\mathbf{u}}_{i+1}$ are column vectors, and $\mathbf{U}_i$ is a square matrix whose dimension is smaller than that of $\mathbf{A}_i$ by one. Since $\mathbf{A}_i$ is a Hermitian matrix, we can write its inverse as

$$\mathbf{A}_i^{-1} = \begin{bmatrix} v_i & \mathbf{v}_i^H \\ \mathbf{v}_i & \mathbf{V}_i \end{bmatrix} \tag{51}$$

where v_i is a scalar, $\mathbf{v}_i$ is a column vector, and $\mathbf{V}_i$ is a square matrix with dimension smaller than that of $\mathbf{A}_i^{-1}$ by one. From the block matrix inversion formula [42], we can obtain $\mathbf{A}_{i+1}^{-1}$ from $\mathbf{A}_i^{-1}$ with the following formula:

$$\mathbf{A}_{i+1}^{-1} = \begin{bmatrix} \mathbf{U}_i^{-1} + \widetilde{\mathbf{b}}_{i+1} \widetilde{\mathbf{b}}_{i+1}^H \widetilde{\beta}_{i+1} & \widetilde{\mathbf{b}}_{i+1} \widetilde{\beta}_{i+1} \\ \widetilde{\mathbf{b}}_{i+1}^H \widetilde{\beta}_{i+1} & \widetilde{\beta}_{i+1} \end{bmatrix} \tag{52}$$

where $\widetilde{\beta}_{i+1} = (\widetilde{u}_{i+1} - \widetilde{\mathbf{u}}_{i+1}^H \mathbf{U}_i^{-1} \widetilde{\mathbf{u}}_{i+1})^{-1}$, $\widetilde{\mathbf{b}}_{i+1} = -\mathbf{U}_i^{-1} \widetilde{\mathbf{u}}_{i+1}$, and

$$\mathbf{U}_i^{-1} = \mathbf{V}_i - \frac{\mathbf{v}_i \mathbf{v}_i^H}{v_i}. \tag{53}$$

For $i = 0, 1, \ldots, D - 1$, $\mathbf{A}_{i+1}$ includes $\mathbf{A}_i$ as its submatrix. We then have

$$\mathbf{A}_{i+1} = \begin{bmatrix} \mathbf{A}_i & \widetilde{\mathbf{u}}_{i+1} \\ \widetilde{\mathbf{u}}_{i+1}^H & \widetilde{u}_{i+1} \end{bmatrix}. \tag{54}$$

Consequently, $\mathbf{A}_{i+1}^{-1}$ can be obtained by (52), where $\mathbf{U}_i^{-1} = \mathbf{A}_i^{-1}$. For $i = N - D, \ldots, N - 1$, $\mathbf{A}_i$ becomes a submatrix of $\mathbf{A}_{i-1}$, which is given by

$$\mathbf{A}_{i-1} = \begin{bmatrix} s_i & \mathbf{s}_i^H \\ \mathbf{s}_i & \mathbf{A}_i \end{bmatrix}. \tag{55}$$

Thus, $\mathbf{A}_i^{-1}$ can be obtained with (53) as follows:

$$\mathbf{A}_i^{-1} = \mathbf{V}_{i-1} - \frac{\mathbf{v}_{i-1} \mathbf{v}_{i-1}^H}{v_{i-1}}. \tag{56}$$

Thus, we only have to conduct one matrix inversion explicitly, i.e., $\mathbf{A}_0^{-1}$, and its dimension is $(D + 1) \times (D + 1)$.

To further reduce the complexity, we can make an approximation when calculating $a_{i,j}$. From the definition, we have $a_{i,j} = \sum_{n=0}^{N-1} \widetilde{m}_{i,n}^* \widetilde{m}_{j,n}$. We can reduce the number of terms included in the summation. We let $a_{i,j} \approx \sum_{n \in \Omega} \widetilde{m}_{i,n}^* \widetilde{m}_{j,n}$, where $\Omega = \langle i - S : i + S, N \rangle \cap \langle j - S : j + S, N \rangle$, and S is the number of one-sided ICI terms taken into consideration ($0 \le S \le N/2 - 1$). The notation $\langle i : j, N \rangle$ denotes a sequence of $\{i - N\lfloor i/N \rfloor, i + 1 - N\lfloor (i+1)/N \rfloor, \ldots, j -$

$N\lfloor j/N \rfloor\}$ (here, i and j are integers and $i \le j$). With this approach, $a_{i,j}$ is approximately evaluated, and so is $\mathbf{A}_i$ in (39). The value of S then determines the accuracy of the solution in (39). A small S can greatly reduce the complexity but results in low accuracy of the solution. Recall that ICI on a subcarrier mainly comes from a few neighboring subcarriers. As a result, we can always find a small S affecting the final result only slightly. For the determination of S, it depends on the value of ICI; the larger the ICI, the larger S we should use. In our simulations, the largest S that we use is two.

As mentioned, if $D = 0$, $\mathbf{W}_0$ will become a diagonal matrix. In this case, the initial values can be approximated as

$$w_{i,i} \approx \frac{\widetilde{m}_{i,i}^*}{\sum_{n \in \Omega'} |\widetilde{m}_{i,n}|^2} \tag{57}$$

where $\Omega' = \langle i - S : i + S, N \rangle$. There is an interesting property in (57). If we take only the diagonal terms of the ICI matrix into account (i.e., $S = 0$), the initial values will degenerate into the coefficients of the conventional one-tap FEQ. If there is no ICI, Newton's iteration with (57) will stop after initialization ($k = 0$).

APPENDIX B
DERIVATION OF THE INITIAL VALUE FOR MIMO-OFDM SYSTEMS

As we did in the SISO-OFDM systems, we use the minimum-Frobenius-norm criterion to obtain the initial value. Note that the initial matrix for the MIMO-OFDM scenario is no longer a banded matrix. Instead, it is a matrix composed of four banded submatrices. Let $\alpha_{i,j} = \mathbf{W}_\alpha(i,j)$, $\beta_{i,j} = \mathbf{W}_\beta(i,j)$, $\gamma_{i,j} = \mathbf{W}_\gamma(i,j)$, and $\omega_{i,j} = \mathbf{W}_\omega(i,j)$. Furthermore, define $q_{i,j} = \sum_{n=0}^{N-1} (\widetilde{a}_{i,n}^* \widetilde{a}_{j,n} + \widetilde{b}_{i,n}^* \widetilde{b}_{j,n})$, $r_{i,j} = \sum_{n=0}^{N-1} (\widetilde{c}_{i,n}^* \widetilde{c}_{j,n} + \widetilde{d}_{i,n}^* \widetilde{d}_{j,n})$, and $s_{i,j} = \sum_{n=0}^{N-1} (\widetilde{a}_{i,n}^* \widetilde{c}_{j,n} + \widetilde{b}_{i,n}^* \widetilde{d}_{j,n})$, where $\widetilde{a}_{i,j} = \widetilde{\mathbf{M}}_{1,1}(i,j)$, $\widetilde{b}_{i,j} = \widetilde{\mathbf{M}}_{1,2}(i,j)$, $\widetilde{c}_{i,j} = \widetilde{\mathbf{M}}_{2,1}(i,j)$, and $\widetilde{d}_{i,j} = \widetilde{\mathbf{M}}_{2,2}(i,j)$. It turns out that we can obtain the optimum initial values by solving the following equation:

$$\mathbf{T}_i \mathbf{b}_i = \mathbf{c}_i, \qquad i = 0, 1, \ldots, 2N - 1 \tag{58}$$

where $\mathbf{b}_i$ is the ith row of the optimum $\mathbf{W}_0$. Definitions of $\mathbf{T}_i$, $\mathbf{b}_i$, and $\mathbf{c}_i$ may be different for different i's. Note that we have two sets of banded matrices to deal with: One is for $i = 0, 1, \ldots, N - 1$, and the other is for $i = N, N + 1, \ldots, 2N - 1$. We then need to consider three cases for each set. Fortunately, they are similar. For the set of $i = 0, 1, \ldots, N - 1$, we have the following.

1) For $i = D, D + 1, \ldots, N - 1 - D$, we have

$$\mathbf{T}_i = \begin{bmatrix} \mathbf{Q}_i & \mathbf{S}_i \\ \mathbf{S}_i^H & \mathbf{R}_i \end{bmatrix} \tag{59}$$

$$\mathbf{Q}_i = \begin{bmatrix} q_{i-D,i-D} & \cdots & q_{i-D,i+D} \\ \vdots & \ddots & \vdots \\ q_{i+D,i-D} & \cdots & q_{i+D,i+D} \end{bmatrix} \tag{60}$$

$$\mathbf{b}_i = [\alpha_{i,i-D}, \ldots, \alpha_{i,i+D}, \beta_{i,i-D}, \ldots, \beta_{i,i+D}]^T \tag{61}$$

$$\mathbf{c}_i = [\widetilde{a}_{i-D,i}^*, \ldots, \widetilde{a}_{i+D,i}^*, \widetilde{c}_{i-D,i}^*, \ldots, \widetilde{c}_{i+D,i}^*]^T. \tag{62}$$

Matrices $\mathbf{R}_i$ and $\mathbf{S}_i$ can be obtained by replacing $q_{m,n}$ in $\mathbf{Q}_i$ with $r_{m,n}$ and $s_{m,n}$, respectively.

2) For $i = 0, 1, \ldots, D - 1$, we have

$$\mathbf{T}_i = \begin{bmatrix} \mathbf{Q}_i & \mathbf{S}_i \\ \mathbf{S}_i^H & \mathbf{R}_i \end{bmatrix} \tag{63}$$

$$\mathbf{Q}_i = \mathbf{Q}_D(0 : D + i, 0 : D + i) \tag{64}$$

$$\mathbf{R}_i = \mathbf{R}_D(0 : D + i, 0 : D + i) \tag{65}$$

$$\mathbf{S}_i = \mathbf{S}_D(0 : D + i, 0 : D + i) \tag{66}$$

$$\mathbf{b}_i = [\alpha_{i,0}, \ldots, \alpha_{i,i+D}, \beta_{i,0}, \ldots, \beta_{i,i+D}]^T \tag{67}$$

$$\mathbf{c}_i = \left[\widetilde{a}_{0,i}^*, \ldots, \widetilde{a}_{i+D,i}^*, \widetilde{c}_{0,i}^*, \ldots, \widetilde{c}_{i+D,i}^* \right]^T. \tag{68}$$

3) For $i = N - D, N - D + 1, \ldots, N - 1$, we have

$$\mathbf{T}_i = \begin{bmatrix} \mathbf{Q}_i & \mathbf{S}_i \\ \mathbf{S}_i^H & \mathbf{R}_i \end{bmatrix} \tag{69}$$

$$\mathbf{Q}_i = \mathbf{Q}_{N-1-D}(i - N + 1 + D : 2D, \quad i - N + 1 + D : 2D) \tag{70}$$

$$\mathbf{R}_i = \mathbf{R}_{N-1-D}(i - N + 1 + D : 2D, \quad i - N + 1 + D : 2D) \tag{71}$$

$$\mathbf{S}_i = \mathbf{S}_{N-1-D}(i - N + 1 + D : 2D, \quad i - N + 1 + D : 2D) \tag{72}$$

$$\mathbf{b}_i = [\alpha_{i,i-D}, \ldots, \alpha_{i,N-1}, \beta_{i,i-D}, \ldots, \beta_{i,N-1}]^T \tag{73}$$

$$\mathbf{c}_i = \left[\widetilde{a}_{i-D,i}^*, \ldots, \widetilde{a}_{N-1,i}^*, \widetilde{c}_{i-D,i}^*, \ldots, \widetilde{c}_{N-1,i}^* \right]^T. \tag{74}$$

Note that $\mathbf{Q}_i$, $\mathbf{R}_i$, and $\mathbf{S}_i$ in the second case correspond to the upper left submatrices of $\mathbf{Q}_D$, $\mathbf{R}_D$, and $\mathbf{S}_D$, respectively. In addition, $\mathbf{Q}_i$, $\mathbf{R}_i$, and $\mathbf{S}_i$ in the third case correspond to the lower right submatrices of $\mathbf{Q}_{N-1-D}$, $\mathbf{R}_{N-1-D}$, and $\mathbf{S}_{N-1-D}$, respectively.

For $i = N, N + 1, \ldots, 2N - 1$, we can use the same equations shown in (59)–(74). However, we have to let $\mathbf{T}_i = \mathbf{T}_{i-N}$ and replace $\alpha_{i,j}$ and $\beta_{i,j}$ in $\mathbf{b}_i$ with $\gamma_{i,j}$ and $\omega_{i,j}$, respectively, and $\widetilde{a}_{i,j}^*$ and $\widetilde{c}_{i,j}^*$ in $\mathbf{c}_i$ with $\widetilde{b}_{i,j}^*$ and $\widetilde{d}_{i,j}^*$, respectively. Since the initial matrix is no longer a banded matrix, we are not able to obtain a recursive relationship in solving (58). Gaussian elimination may be a good choice for this problem. As mentioned, $\mathbf{T}_i = \mathbf{T}_{i-N}$; we need only to construct $\mathbf{T}_i$ and perform Gaussian elimination of $\mathbf{T}_i$ for $i = 0, 1, \ldots, N - 1$ once. Furthermore, $\mathbf{T}_i$ is a Hermitian matrix, making Gaussian elimination even less complex.

To further reduce the computational complexity, we can make some approximations in the calculation of $q_{i,j}$, $r_{i,j}$, and $s_{i,j}$. We can let $q_{i,j} \approx \sum_{n \in \Omega} (\widetilde{a}_{i,n}^* \widetilde{a}_{j,n} + \widetilde{b}_{i,n}^* \widetilde{b}_{j,n})$, $r_{i,j} \approx \sum_{n \in \Omega} (\widetilde{c}_{i,n}^* \widetilde{c}_{j,n} + \widetilde{d}_{i,n}^* \widetilde{d}_{j,n})$, and $s_{i,j} \approx \sum_{n \in \Omega} (\widetilde{a}_{i,n}^* \widetilde{c}_{j,n} + \widetilde{b}_{i,n}^* \widetilde{d}_{j,n})$, where $\Omega = \langle i - S : i + S, N \rangle \cap \langle j - S : j + S, N \rangle$. Again, this approximation makes use of the property that elements in $\widetilde{\mathbf{M}}_{i,j}$ close to the main diagonal have larger values than the others.

REFERENCES

[1] J. A. C. Bingham, "Multicarrier modulation for data transmission: An idea whose time has come," *IEEE Commun. Mag.*, vol. 28, no. 5, pp. 5–14, May 1990.

[2] M. Russell and G. L. Stüber, "Interchannel interference analysis of OFDM in a mobile environment," in *Proc. IEEE VTC*, Jul. 25–28, 1995, vol. 2, pp. 820–824.

[3] P. Robertson and S. Kaiser, "The effects of Doppler spreads in OFDM(A) mobile radio systems," in *Proc. IEEE VTC—Fall*, Sep. 19–22, 1999, vol. 1, pp. 329–333.

[4] Y. Li and L. J. Cimini, Jr., "Bounds on the interchannel interference of OFDM in time-varying impairments," *IEEE Trans. Commun.*, vol. 49, no. 3, pp. 401–404, Mar. 2001.

[5] J. Li and M. Kavehrad, "Effects of time selective multipath fading on OFDM systems for broadband mobile applications," *IEEE Commun. Lett.*, vol. 3, no. 12, pp. 332–334, Dec. 1999.

[6] H. Steendam and M. Moeneclaey, "Analysis and optimization of the performance of OFDM on frequency-selective time-selective fading channels," *IEEE Trans. Commun.*, vol. 47, no. 12, pp. 1811–1819, Dec. 1999.

[7] Y. Zhang and H. Liu, "MIMO-OFDM systems in the presence of phase noise and doubly selective fading," *IEEE Trans. Veh. Technol.*, vol. 56, no. 4, pp. 2277–2285, Jul. 2007.

[8] W. G. Jeon, K. H. Chang, and Y. S. Cho, "An equalization technique for orthogonal frequency-division multiplexing systems in time-variant multipath channels," *IEEE Trans. Commun.*, vol. 47, no. 1, pp. 27–32, Jan. 1999.

[9] Y.-S. Choi, P. J. Voltz, and F. A. Cassara, "On channel estimation and detection for multicarrier signals in fast and selective Rayleigh fading channels," *IEEE Trans. Commun.*, vol. 49, no. 8, pp. 1375–1387, Aug. 2001.

[10] X. Cai and G. B. Giannakis, "Bounding performance and suppressing intercarrier interference in wireless mobile OFDM," *IEEE Trans. Commun.*, vol. 51, no. 12, pp. 2047–2056, Dec. 2003.

[11] W.-S. Hou and B.-S. Chen, "ICI cancellation for OFDM communication systems in time-varying multipath fading channels," *IEEE Trans. Wireless Commun.*, vol. 4, no. 5, pp. 2100–2110, Sep. 2005.

[12] A. Gorokhov and J.-P. Linnartz, "Robust OFDM receivers for dispersive time-varying channels: Equalization and channel acquisition," *IEEE Trans. Commun.*, vol. 52, no. 4, pp. 572–583, Apr. 2004.

[13] S. Tomasin, A. Gorokhov, H. Yang, and J.-P. Linnartz, "Iterative interference cancellation and channel estimation for mobile OFDM," *IEEE Trans. Wireless Commun.*, vol. 4, no. 1, pp. 238–245, Jan. 2005.

[14] X. Huang and H.-C. Wu, "Robust and efficient intercarrier interference mitigation for OFDM systems in time-varying fading channels," *IEEE Trans. Veh. Technol.*, vol. 56, no. 5, pp. 2517–2528, Sep. 2007.

[15] W.-G. Song and J.-T. Lim, "Channel estimation and signal detection for MIMO-OFDM with time varying channels," *IEEE Commun. Lett.*, vol. 10, no. 7, pp. 540–542, Jul. 2006.

[16] Y. Zhao and S.-G. Haggman, "Intercarrier interference self-cancellation scheme for OFDM mobile communication systems," *IEEE Trans. Commun.*, vol. 49, no. 7, pp. 1185–1191, Jul. 2001.

[17] Y. Zhang and H. Liu, "Frequency-domain correlative coding for MIMO-OFDM systems over fast fading channels," *IEEE Commun. Lett.*, vol. 10, no. 5, pp. 347–349, May 2006.

[18] K. W. Park and Y. S. Cho, "An MIMO-OFDM technique for high-speed mobile channels," *IEEE Commun. Lett.*, vol. 9, no. 7, pp. 604–606, Jul. 2005.

[19] S. Das and P. Schniter, "Beamforming and combining strategies for MIMO-OFDM over doubly selective channels," in *Proc. IEEE ACSSC*, Oct./Nov. 2006, pp. 804–808.

[20] A. Stamoulis, S. N. Diggavi, and N. Al-Dhahir, "Intercarrier interference in MIMO OFDM," *IEEE Trans. Signal Process.*, vol. 50, no. 10, pp. 2451–2464, Oct. 2002.

[21] I. Barhumi, G. Leus, and M. Moonen, "Equalization for OFDM over doubly selective channels," *IEEE Trans. Signal Process.*, vol. 54, no. 4, pp. 1445–1458, Apr. 2006.

[22] I. Barhumi, G. Leus, and M. Moonen, "Time-varying FIR equalization for doubly selective channels," *IEEE Trans. Wireless Commun.*, vol. 4, no. 1, pp. 202–214, Jan. 2005.

[23] I. Barhumi, G. Leus, and M. Moonen, "Time-domain and frequency-domain per-tone equalization for OFDM over doubly selective channels," *Signal Process.*, vol. 84, no. 11, pp. 2055–2066, Nov. 2004.

[24] K. Van Acker, G. Leus, M. Moonen, O. van de Wiel, and T. Pollet, "Per tone equalization for DMT-based systems," *IEEE Trans. Commun.*, vol. 49, no. 1, pp. 109–119, Jan. 2001.

[25] G. Leus and M. Moonen, "Per-tone equalization for MIMO OFDM systems," *IEEE Trans. Signal Process.*, vol. 51, no. 11, pp. 2965–2975, Nov. 2003.

[26] P. Schniter, "Low-complexity equalization of OFDM in doubly selective channels," *IEEE Trans. Signal Process.*, vol. 52, no. 4, pp. 1002–1011, Apr. 2004.

[27] X. Qian and L. Zhang, "Interchannel interference cancellation in wireless OFDM systems via Gauss–Seidel method," in *Proc. IEEE ICCT*, Apr. 9–11, 2003, pp. 1051–1055.

[28] A. F. Molisch, M. Toeltsch, and S. Vermani, "Iterative methods for cancellation of intercarrier interference in OFDM systems," *IEEE Trans. Veh. Technol.*, vol. 56, no. 4, pp. 2158–2167, Jul. 2007.

[29] Y. Mostofi and D. C. Cox, "ICI mitigation for pilot-aided OFDM mobile systems," *IEEE Trans. Wireless Commun.*, vol. 4, no. 2, pp. 765–774, Mar. 2005.

[30] J. Fu, C.-Y. Pan, Z.-X. Yang, and L. Yang, "Low-complexity equalization for TDS-OFDM systems over doubly selective channels," *IEEE Trans. Broadcast.*, vol. 51, no. 3, pp. 401–407, Sep. 2005.

[31] G. H. Golub and C. F. Van Loan, *Matrix Computations*. London, U.K.: Johns Hopkins Univ. Press, 1996.

[32] C.-Y. Hsu and W.-R. Wu, "A low-complexity ICI mitigation method for high-speed mobile OFDM systems," in *Proc. IEEE ISCAS*, May 21–24, 2006, pp. 4511–4514.

[33] G. Schulz, "Iterative berechnung der reziproken matrix," *Z. Angew. Math. Mech.*, vol. 13, pp. 57–59, 1933.

[34] A. S. Householder, *The Theory of Matrix in Numerical Analysis*. New York: Dover, 1964.

[35] A. Ben-Israel, "A note on iterative method for generalized inversion of matrices," *Math. Comput.*, vol. 20, no. 95, pp. 439–440, Jul. 1966.

[36] A. Ben-Israel and D. Cohen, "On iterative computation of generalized inverses and associated projections," *SIAM J. Numer. Anal.*, vol. 3, no. 3, pp. 410–419, Sep. 1966.

[37] V. Y. Pan and R. Schreiber, "An improved Newton iteration for the generalized inverse of a matrix, with applications," *SIAM J. Sci. Stat. Comput.*, vol. 12, no. 5, pp. 1109–1130, Sep. 1991.

[38] V. Y. Pan and J. Reif, "Fast and efficient parallel solution of dense linear systems," *Comput. Math. Appl.*, vol. 17, no. 11, pp. 1481–1491, 1989.

[39] V. Y. Pan, Y. Rami, and X. Wang, "Structured matrices and Newton's iteration: Unified approach," *Linear Algebra Appl.*, vol. 343/344, pp. 233–265, Mar. 2002.

[40] S. J. Leon, *Linear Algebra With Applications*. Englewood Cliffs, NJ: Prentice–Hall, 1998.

[41] M. F. Pop and N. C. Beaulieu, "Limitations of sum-of-sinusoids fading channel simulators," *IEEE Trans. Commun.*, vol. 49, no. 4, pp. 699–708, Apr. 2001.

[42] D. A. Harville, *Matrix Algebra From a Statistician's Perspective*. New York: Springer-Verlag, 1997.

Chao-Yuan Hsu (S'08) received the B.S. degree in electrical engineering in 1999 from National Sun Yat-Sen University, Kaohsiung, Taiwan, and the M.S. degree in communication engineering in 2003 from National Chiao Tung University, Hsinchu, Taiwan, where he is currently working toward the Ph.D. degree in communication engineering within the Department of Communication Engineering.

His research interests include intercarrier interference cancellation in orthogonal frequency division multiplexing-based systems and digital communication.

Wen-Rong Wu (M'89) received the B.S. degree in mechanical engineering from Tatung Institute of Technology, Taipei, Taiwan, in 1980 and the M.S. degree in mechanical engineering in 1985, the M.S. degree in electrical engineering in 1986, and the Ph.D. degree in electrical engineering in 1989 from the State University of New York, Buffalo.

Since August 1989, he has been a faculty member with the Department of Communication Engineering, National Chiao Tung University, Hsinchu, Taiwan. His research interests include statistical signal processing and digital communication.